EPR SPECTROSCOPIC AND QUANTUM CHEMICAL STUDIES OF SOME INORGANIC MAIN GROUP RADICALS

HEIKKI M. TUONONEN
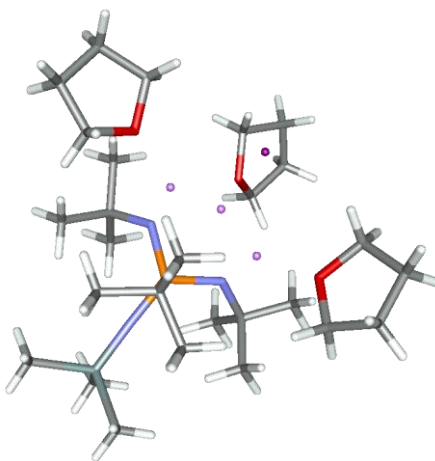
Academic Dissertation
for the Degree of
Doctor of Philosophy

Jyväskylä, Finland 2005

EPR SPECTROSCOPIC AND
QUANTUM CHEMICAL STUDIES OF SOME
INORGANIC MAIN GROUP RADICALS

BY

HEIKKI M. TUONONEN

Academic Dissertation

for the Degree of

Doctor of Philosophy

To be presented, by permission of the Faculty of Mathematics and Science of the

University of Jyväskylä, for public examination in Blomstedt Auditorium,

on December 2nd, 2005, at 12 noon.

To my Dad

Preface

The work reviewed in this thesis was carried out between the summers 2001 and 2005 at the Departments of Chemistry, University of Jyväskylä and University of Calgary. In both places, I had the privilege to work in excellent research environments for which I am grateful to the co-workers and personnel at these Departments.
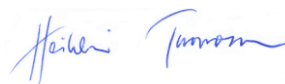
I wish to express my warmest gratitude to my supervisors Prof. Risto Laitinen, Jussi Valkonen, and Tristram Chivers, as well as Doc. Reijo Suontamo for the support, criticism, and suggestions they have given me in the past years. I am indebted to them for so much that it would be pointless to try to encapsulate it any further. My compliments also go to Prof. René Boeré for tutoring me in the fine art of EPR spectroscopy and being an honourable opponent in chemical discussions.

I am also thankful for my fellow Graduate Students MSc. Mikko Rautiainen, Dr. Andrea Armstrong, and MSc. Tracey Roemmele, who among all people have suffered the most from my bad jokes by sharing office space with me. Thank you for the refreshing discussions and arguments about everything from the mundane daily life to the line of Merovingian kings which, along with the freshly brewed coffee, created an extremely pleasant working atmosphere. Extra special thanks goes to Andrea for the numerous helpful discussions about the language and contents of the preparatory manuscript of this thesis.

As people before me have described, writing a thesis is similar to entering a long-term relationship with an obsessive partner: it demands nearly constant attention to the exclusion of everything else. I remain ever grateful to my wife Nuppu who has been remarkably patient and supportive throughout the four and a half years, and especially during the last three months of intense writing. Thank you for putting up with my late hours, my spoiled weekends, and my sometimes not-so-good temper. Above all, thank you for loving me and surviving the ordeal.

Jyväskylä, September 15th 2005

v

Abstract

The study of radicals is a fascinating undertaking that, through a combination of structural studies, electron paramagnetic resonance spectroscopy, and quantum chemical calculations, provides informative insights into the electronic structures in odd-electron systems. In the present dissertation, quantum chemical methods have been used to aid in the interpretation of experimental observations gathered for a number of main group radicals. A theoretical analysis of the electronic structures of some inorganic diradicaloids is also presented. A detailed understanding of the molecular and electronic structures of these systems, and the factors which govern them, is essential for future studies of their incorporation into useful materials.

The research presented in the first half of this thesis describes the synthesis and characterization of new stable radicals of the main group elements. It resulted in the preparation of multiple stable and persistent systems incorporating the tetraimidophosphate dianion radical $\{Li_2[P(N^tBu)_3(NSiMe_3)]\}^\bullet$, as well as in the synthesis of the first stable metal complexes of the boraamidinato radical $\{[PhB(N^tBu)_2]^-\}^\bullet$. The spectroscopic and density functional studies described herein played a crucial role in the characterization of these novel paramagnetic species. The results from theoretical calculations on some stable paramagnetic complexes of the 1,4-diaza-1,3-butadiene ligand with gallium are also presented. The computational data provided valuable information aiding the interpretation of their EPR spectra as well as the analysis of the solution behaviour of some related radical species.

The second half of this thesis summarizes the key findings from theoretical investigations of the electronic structures of some main group singlet diradicaloids. The results reveal that, despite opposed claims, stable main group singlet diradicaloids with significant amounts of diradical character still await their discovery. The quantum chemical calculations also demonstrate the importance of correct theoretical description of static electron correlation effects in these systems, and provide high-level computational data which can be used in the experimental efforts focused on the preparation of the conducting polymers $(SeN)_x$ and $(SeNSN)_x$.

List of original publications

This thesis is based on the following original research papers:

I   **Cubic and Spirocyclic Radicals Containing a Tetraimidophosphate Dianion [P(NR)₃(NR')]•²⁻**, Andrea F. Armstrong, Tristram Chivers, Heikki M. Tuononen, Masood Parvez, and René T. Boeré, *Inorg. Chem.*, **2005**, *44*, 7981−7991.

The author of the present thesis has performed all the computational work reported in the paper; the experimental work was conducted by A. F. Armstrong. The EPR spectral simulations and analyses reported in the paper were done by A. F. Armstrong and the author. The author has also written a part of the paper. https://doi.org/10.1021/ic051128q

II   **Synthesis and Structures of Aluminum and Magnesium Complexes of Tetraimidophosphates and Trisamidothiophosphates: EPR and DFT Investigations of the Persistent Neutral Radicals {Me₂Al[(μ-NR)(μ-NᵗBu)]P(μ-NᵗBu)₂]Li(THF)₂}• (R = SiMe₃, ᵗBu)**, Andrea Armstrong, Tristram Chivers, Heikki M. Tuononen, and Masood Parvez, *Inorg. Chem.*, **2005**, *44*, 5778−5788.

The author of the present thesis has performed all the computational work reported in the paper; the experimental work was conducted by A. Armstrong. The EPR spectral simulations and analyses reported in the paper were done by A. Armstrong and the author. The author has also written a part of the paper.

https://doi.org/10.1021/ic050689e

III   **Stable Spirocyclic Neutral Radicals: Aluminium and Gallium Boraamidinates**, Tristram Chivers, Dana J. Eisler, Chantall Fedorchuk, Gabriele Schatte, Heikki M. Tuononen, and René T. Boeré, *Chem. Commun.*, **2005**, 3930−3932.

The author of the present thesis has performed all the computational work reported in the paper; the experimental work was conducted by C. Fedorchuk. The EPR spectral simulations and analyses reported in the paper were done by A. F. Armstrong and the author. The author has also co-written the paper. https://doi.org/10.1039/B506253E

IV **Theoretical Investigation of Paramagnetic Diazabutadiene Gallium(III)-Pnictogen Complexes: Insights into the Interpretation and Simulation of Electron Paramagnetic Resonance Spectra**, Heikki M. Tuononen and Andrea F. Armstrong, *Inorg. Chem.*, **2005**, *44*, 8277−8284.

The author of the present thesis has performed all the computational work and EPR spectral simulations reported in the paper. The author has also co-written the paper.

V **Electronic Structures and Spectroscopic Properties of 6π-Electron Ring Molecules and Ions E_2N_2 and E_4^{2+} (E = S, Se, Te)**, Heikki M. Tuononen, Reijo Suontamo, Jussi Valkonen, and Risto S. Laitinen, *J. Phys. Chem. A*, **2004**, *108*, 5670−5677.

The author of the present thesis has performed all the quantum chemical calculations reported in the paper and is the principal writer of the paper.

VI **Electronic Structures and Molecular Properties of Chalcogen Nitrides Se_2N_2 and $SeSN_2$**, Heikki M. Tuononen, Reijo Suontamo, Jussi Valkonen, Risto S. Laitinen, and Tristram Chivers, *J. Phys. Chem. A*, **2005**, *109*, 6309−6317.

The author of the present thesis has performed all the quantum chemical calculations reported in the paper and is the principal writer of the paper.

Contents

Chapter 1

Introduction

Ever since their discovery in the turn of the 20th century, stable radicals have fascinated researchers. Their existence presents a clear contradiction to the classic tenet in chemistry that molecules with open-shell configurations are transient or highly reactive species. From a fundamental perspective, the study of these systems is important not only because they challenge our conventional chemical thinking, but because they develop our understanding of molecular structure and bonding. The recent syntheses of several stable singlet diradicaloids are particularly important in this regard.[1] In addition, the paramagnetic nature of stable radicals renders them useful in several applications; among other things, radicals can be used as molecular spin-labels,[2] polymerization catalysis,[3] and reagents in redox chemistry.[4] There is also a growing interest in the biological activity of radicals[5] and in the electronic and magnetic properties of molecule-based materials utilizing stable radicals as building blocks.[6]

The aim of the present study has been twofold: first, to synthesize and characterize new stable main group radicals, and, second, to provide a deeper understanding of the electronic structures of some valence isoelectronic main group singlet diradicaloids. The emphasis in the first objective was on the interplay of experimental and theoretical methods in elucidating the molecular and electronic structures of odd-electron species; in the second objective, high-level quantum chemical methods were used to unravel the significance of singlet diradical character in some

selected systems for the prediction of their molecular properties. On the whole, through a combined use of different methodologies, this work yielded a profound understanding of main group radicals which is essential for future investigations of their usage in various applications such as molecule-based magnets or paramagnetic thin films.

Chapter 2

Stable main group radicals

Though stable[i] radical chemistry has a long history dating back to Gomberg's discovery of the triphenymethyl radical $^{\bullet}CPh_3$ in 1900,[7] major advances in the synthesis and characterization of stable and persistent main group radicals have been made during the past decades.[8] Much to the chemists' dismay, the synthesis of main group radicals is problematical due to the smaller number of degenerate orbitals present in the complexes of p-block elements as compared to those of transition metals. In addition, main group molecules with partially filled valence orbitals are usually susceptible to association with either electron donors or acceptors. Despite these obstacles, an ever-increasing number of stable or persistent odd-electron species of the main group elements are being reported in the literature.[9] Such species are primarily stabilized either by delocalization of the unpaired electron(s) over electronegative atoms, or by kinetic stabilization using bulky substituents, or by a combination of these two effects. Although only a small proportion of the reported systems have yet been of practical importance, the sheer number of published experimental results demonstrates that the allure of stable radicals has not diminished much since their initial discovery.

---

[i] The term "stable", as applied to radicals, is taken to indicate "a species that can be isolated and shows no sign of decomposition under an inert atmosphere at room temperature", whereas a "persistent" radical has "a relatively long lifetime under the conditions it is generated". Radicals which do not fall into either of these categories, that is, those with half-lives of less than minutes, are referred to as "transient".[8]

Many stable main group radicals exhibit a delocalization of spin density over a π-manifold comprising of second- and third-row elements common in organic compounds, *i.e.* C, N, O, and S. A considerably smaller number of examples of stable and persistent main group systems in which the unpaired electron(s) is (are) localized primarily on the heavier main group atoms exist;[8b] it was not until the mid-1970s that the first examples of such species were synthesized and characterized in solution.[10] Even today only a handful of examples of radicals in which the spin density is localized on the group 15 and 16 elements As, Sb, Se, or Te are known.[8b] In addition, especially in group 13 and 16 chemistry, many of the so-called stable radicals are obtained as charged species, that is, they are isolated in salts as either anion or cation radicals.[8b] Much of the recent research interest has therefore focussed on the synthesis of *neutral* main group radicals incorporating heavier p-block elements that would be stable at room temperature.

Electron paramagnetic resonance (EPR) spectroscopy has long been the single most important experimental method used in the characterization and study of radicals, as the hyperfine coupling of the unpaired electron(s) to the different magnetically active nuclei gives important information regarding its location within a molecule. Other experimental techniques such as electron-nuclear double resonance (ENDOR) spectroscopy, X-ray crystallography, and cyclic voltammetry have also been used. During the last decade, theoretical methods have become as important research tools for the study of radicals as their experimental counterparts.[11] This stems mainly from the developments in density functional theory (DFT) which have made semi-quantitative studies of electronic structures of radicals comprising of hundreds of atoms routine.[12] In addition, advances in wave function-based methods have allowed radicals with tens of atoms to be studied with unparalleled accuracy.[13] Improvements in approximate relativistic methods especially in the realm of DFT have also provided access to accurate computational studies of systems incorporating the heavier elements of the p-block.[14] In consequence, a combined approach comprising both experimental and theoretical methods has been adopted in the recent years, which has greatly facilitated the intellectual design of stable radicals and provided deeper understanding of structure-property relationships in odd-electron systems.

The original research Papers **I–III** describe the synthesis and characterization of novel stable and persistent radicals of the p-block elements, whereas Paper **IV** reports computational studies on various paramagnetic complexes of the 1,4-diaza-1,3-butadiene ligands with gallium.

2.1 Electron paramagnetic resonance spectroscopy

EPR spectroscopy[ii] is concerned with microwave-induced transitions (10^9–10^{11} Hz) between magnetic energy levels of electrons having a net spin and orbital angular momentum. The two paramagnetic resonance effects of most importance are the electronic Zeeman and hyperfine interactions. In the following, a concise theoretical treatment of these effects is given for systems with one unpaired electron.[15] EPR spectroscopy was used in the characterization of radicals reported in Papers **I–III**. In Paper **IV**, extant EPR spectroscopic data was re-interpreted in light of results from DFT calculations.

2.1.1 Electronic Zeeman interaction

In the absence of any magnetic field, the magnetic moment associated with the electron spin is randomly oriented and the two energy levels associated with the spin states α and β are degenerate. The application of an external magnetic field $\boldsymbol{B}$ results in a separation of the energy levels as the orientation of electron spin $\boldsymbol{S}$ with respect to the magnetic field vector is quantized. The potential energy of such a system is described by the spin Hamiltonian[iii]

$$H = \beta_e \boldsymbol{S} \cdot \boldsymbol{g} \cdot \boldsymbol{B}, \tag{2.1}$$

[ii] The term electron paramagnetic resonance (EPR) takes into account contributions from both electron orbital as well as spin angular momentum. In most cases, the observed absorption is due to the spin angular momentum alone and the term electron spin resonance (ESR) is often used; electron magnetic resonance (EMR) is an alternative which is also widely used in the literature.[15]

[iii] The full Hamiltonian operator of a molecular system is a function of the positions and momenta of all particles present (the spatial component), and of their intrinsic angular momenta (the spin component). The quantum mechanical description of magnetic resonance is considerably simplified if the full Hamiltonian operator is averaged over the spatial coordinates and the spin coordinates of the paired electrons. The resulting entity, consisting of parameters and spin operators, is called a spin Hamiltonian, and it gives the same energy levels as the exact Hamiltonian with calculated wave functions.

where β_e is the Bohr magneton and the g-matrix parameterizes the orientational, anisotropic, dependence of the resonance.

Choosing the z axis along $\boldsymbol{B}$ and assuming isotropic behaviour, Equation (2.1) simplifies to

$$H = g\beta_e B S_z. \tag{2.2}$$

Transitions between the two electronic Zeeman levels may be induced by an electromagnetic radiation of the appropriate frequency ν such that the photon energy $h\nu$ matches the energy level separation

$$h\nu = g\beta_e B. \tag{2.3}$$

In practical spectroscopy, the microwave frequency is usually held constant and the magnetic field is swept linearly.

2.1.2   Electronic hyperfine interaction

The electronic Zeeman interaction alone yields an EPR spectrum with only a single line which may be broadened if the $\boldsymbol{g}$-matrix is highly anisotropic. Although there are many examples of systems for which the $\boldsymbol{g}$-matrix (or the isotropic g-value) is distinctive enough to provide a reasonable identification of the paramagnetic species, the resulting EPR spectra would nevertheless be extremely dull.

When one or more magnetically active nuclei in the molecule are able to interact with the unpaired electron, additional terms[iv] need to be included in the spin Hamiltonian. Thus, Equation (2.1) becomes

$$H = \beta_e \boldsymbol{S} \cdot \boldsymbol{g} \cdot \boldsymbol{B} + \boldsymbol{S} \cdot \sum_i \boldsymbol{A}_i \cdot \boldsymbol{I}_i, \tag{2.4}$$

where $\boldsymbol{A}_i$ and $\boldsymbol{I}_i$ are the hyperfine parameter matrix and nuclear spin, respectively, for nucleus i. Again, assuming isotropic behaviour and choosing z axis along $\boldsymbol{B}$, Equation (2.4) simplifies to

---

[iv] In principle, the nuclear Zeeman interaction terms, $\beta_n \sum g_i \boldsymbol{B} \cdot \boldsymbol{I}_i$ should also be included in the spin Hamiltonian. However, in most cases these energy contributions are negligible on the EPR energy scale and cancel out in calculating transition energies.

$$H = g\beta_e B S_z + \sum_i A_i S_z I_{iz},\qquad(2.5)$$

where the factors A_i are called the isotropic hyperfine coupling constants (HFCCs). They measure the magnetic interaction energy between the unpaired electron and the nucleus i.[v]

Two mechanisms with different physical origins contribute to the coupling between electron and nuclear spins. The first mechanism is the dipole-dipole interaction between the magnetic moments of the electron and nuclear spins. This interaction is anisotropic in nature and averages out for example by molecular motion in solution, and will not be discussed further. The second mechanism, called the Fermi contact interaction, becomes important if there is finite electron spin density on any of the interacting magnetically active nuclei. Thus, the Fermi contact term is an *s*-wave contribution because only *s*-orbitals have a non-zero probability density at the nucleus. By virtue of the spherical symmetry of the *s*-orbitals, the Fermi contact interaction is isotropic in nature. The factors A_i, the isotropic HFCCs, in Equation (2.5) are given (in the first-order) by the expression

$$A_i = \frac{8\pi}{3} g_e \beta_e g_i \beta_n \left\langle \Psi \left| \delta(r_i) S_z \right| \Psi \right\rangle = \frac{8\pi}{3} g_e \beta_e g_i \beta_n \rho(r_i),\qquad(2.6)$$

where β_n is the nuclear magneton, g_e is the electronic *g*-factor, and g_i and $\rho(r_i)$ are the nuclear *g*-factor and electron spin density at the nucleus, respectively, for nucleus i. It is noted that according to Equation (2.6), the isotropic HFCCs can be either positive or negative depending on the spin density and the nuclear *g*-value.

It is obvious that the additional terms in the Equation (2.4) compared to the Equation (2.1) increase the number of possible energy levels in the system and, hence, the number of possible transitions. Thus, the EPR signal created by the electronic Zeeman interaction is further split and additional resonances appear in the spectrum at different field strengths. Simply put, the local magnetic fields $\boldsymbol{B}_i$ created by each magnetically active nucleus i in the molecule either oppose or add to the external

---

[v] Though SI-units suitable for reporting HFCCs are Tesla, J, or MHz, a unit of Gauss is in common use in the EPR community and will be used throughout this thesis. Note that 1 G = 0.1 mT.

magnetic field B. When B_i adds to B, a smaller magnetic field strength from the external laboratory magnet is needed to induce a transition and the field for resonance is lowered. The opposite is true when B_i opposes B. In consequence, the observed EPR signal will have a hyperfine structure characteristic to the amount, location, and identity of the magnetically active nuclei in the system.

2.1.3 Energy levels and transitions

In principle, the effective spin Hamiltonian can be written for any system with one (or more) unpaired electron(s) as long as the numbers and identities of the magnetically active nuclei are known.[vi] The energy eigenvalues, however, can be solved exactly (that is, in terms of the parameters g and A) only for the simplest systems such as the $S = I = 1/2$ one electron, one nuclei case. A more practical means to calculating the spin energy levels is to use perturbation theory *i.e.* to separate the spin Hamiltonian into two parts, $H = H_0 + H'$. In this case, the smallest contribution(s) to the energy is (are) treated as a perturbation H' and the eigenfunctions of H_0 are used as a basis for determining the energy corrections arising from H.

The perturbational approach is especially suitable when high magnetic fields are used. In general, for most well-behaved EPR systems perturbation theory applied to the first- and second-orders yields energy levels and transition energies that are sufficiently accurate to explain the experimentally observed spectral features.[vii] In such cases, simple rules (which are not discussed herein) for deciphering the origins of the observed splitting patters exist. In cases where the hyperfine energy is large compared to the electronic Zeeman energy, additional shifts and splittings of transitions can occur. The description of these effects generally requires that the perturbational treatment must be carried out to higher orders. When several inequivalent nuclei have sufficiently large hyperfine interactions that at least third-order terms are required, the relative signs of the HFCCs can be extracted from the experimental spectrum provided that the observed transitions are well resolved.

[vi] In some cases, additional terms such as the nuclear quadrupole term need to be included in the Hamiltonian. Additional coupling terms must naturally also be treated if the system contains more than one unpaired electron.

[vii] The resulting transition energies can also be used to simulate the spectrum provided that values for the parameters g and A are correctly inferred from the experimental data.

2.2 Theoretical methods for calculation of isotropic hyperfine coupling constants

Since many of the p-block elements have at least one naturally occurring spin-active isotope, the EPR spectra of these radicals are often quite complex due to hyperfine interactions of the unpaired electron with several magnetically active nuclei. The resultant poor resolution of these EPR spectra renders it difficult to extract accurate values of the hyperfine coupling constants. Because HFCCs are used to glean information regarding the spin density and spin distribution of the unpaired electron throughout a paramagnetic molecule, this is quite problematic, as it can impede researchers from gaining a thorough understanding of a particular radical system. One approach to overcoming this difficulty is to use theoretical calculations to predict the magnitudes of the HFCCs. This approach was utilized in Papers **I**–**IV** in which the electronic structures and HFCCs of some inorganic main group radicals were calculated with DFT methods.

A good approximation of the isotropic HFCC for a magnetically active nucleus i is given by Equation (2.6) *i.e.* the HFCC for nucleus i is simply the electronic spin density evaluated exactly at the nucleus, multiplied with known constants. This property is extremely difficult to calculate accurately because of its high sensitivity to the quality of the wave function at one point in space; the Dirac delta function $\delta(r_i)$ evaluates the wave function only at the nucleus thus making the property very local. Although alternative approaches that use more global operators than the delta function operator in calculations of the Fermi contact interactions have been presented,[16] none of them have yet found widespread use.

The standard delta function formulation in Equation (2.6) also suggests that the Gaussian basis sets used in the majority of molecular orbital calculations are severely inadequate to be used in calculation of Fermi contact interactions. However, it has been shown that, when properly augmented with tight *s*-functions, the standard Gaussian basis sets can indeed overcome the nuclear cusp problem.[17] An exhaustive number of calculations have also demonstrated that the specifically tailored EPR-III basis sets perform well in DFT calculations,[18] as do the more conventional TZVP,[18b,19] while the IGLO basis sets generally give good magnetic properties with a reasonable basis set size

in wave function-based calculations.[20,viii,21] Nevertheless, Slater-type orbitals are still superior and outperform the conventional Gaussian basis sets in many test cases.[22,ix,23]

In general, the unrestricted self-consistent field (SCF) formalism is in many situations the only reasonable option for evaluation of HFCCs using either wave function or DFT-based methods.[24,25] The restricted open-shell (RO) methods are incapable of accounting for spin polarization effects[x] and therefore cannot be used for calculation of HFCCs for which the effect plays a key role. Unfortunately, the use of unrestricted methods introduces spin contamination in addition to spin polarization into the electron density and properties that depend on it; an analysis of an unrestricted Hartree-Fock (UHF) wave function for a doublet state shows that it also includes terms identical to those in a wave function with a quartet multiplicity. An UHF doublet wave function is therefore not a pure spin state but instead a spin contaminated mixture of states with different multiplicities. Moreover, the terms corresponding to the states with higher multiplicities than the target state give rise to spin polarization effects which are inherently wrong. Thus, spin contamination in the UHF wave function leads to an overestimation of the spin polarization effects.

Removal of the contaminants from the wave function by using projection operators does not result in significant improvements: the resulting spin polarization is usually too small because electron correlation effects are neglected.[26] Thus, the use of correlated levels of wave function theory is requisite for obtaining HFCCs that compare favourably with experimental data. Typically, coupled cluster (CC) methods based on either ROHF or UHF reference determinants are used. They allow a very accurate treatment of systems comprised of less than 20 atoms. In cases where

---

[viii] It is sometimes reported that even the small Pople-type basis sets such as 6-31G* and 6-311G* give hyperfine coupling constants in reasonable agreement with experimental values using both wave function- and DFT-based methods. Such a good performance is usually a result of fortuitous error cancellation, as these basis sets are by all standards insufficient to be used in calculation of hyperfine coupling constants.[21]

[ix] The problems associated with the description of nuclear cusps using Gaussian-type basis functions are most severe when nuclei are treated with a point model. Approximations based on Gaussian-type functions converge much faster for any of the (more realistic) finite-nucleus models.[23]

[x] Spin polarization comprises the effects which result because the interactions between the electrons with equal spins are slightly different from the interactions between electrons having opposite spins (Pauli exclusion principle). As a consequence, in a radical system, two paired electrons from an inner doubly occupied orbital interact somewhat differently with the unpaired electron(s), which results in non-zero spin density also outside of the singly occupied molecular orbital.

multiconfigurational (MC) treatment becomes necessary, multireference configuration interaction (MRCI) generally becomes the method of choice.

Just as in the UHF variant, the unrestricted Slater determinant built from the Kohn-Sham orbitals becomes spin contaminated.[25] However, the Kohn-Sham Slater determinant is not the true wave function of the system (it only describes a hypothetical reference state) and the extent to which spin contamination affects the true wave function cannot be determined. However, it is of some consolation to know that the vast number of calculations performed for doublet radicals have shown that for the majority of unrestricted Kohn-Sham determinants the spin contamination does not play a significant role.[27] For this reason, the unrestricted DFT calculations do not overestimate spin polarization as much as the spin contaminated UHF does, which further leads to more accurate spin densities and, hence, better description of molecular properties that result from this.

For most organic doublet radicals, the spin contamination effect is generally minute and both wave function and Kohn-Sham formalisms using unrestricted reference determinants perform well. However, in the case of transition metal compounds, spin contamination in the unrestricted determinant can be very large for both approaches, rendering the calculated HFCCs dubious.[22,28] A method for the calculation of HFCCs which solves the problems related to spin contamination is the restricted-unrestricted response function approach.[29] It is based on the idea of a spin-restricted unperturbed system which responds to the perturbation, the Fermi contact interaction, in an unrestricted manner. Thus, a proper description of spin polarization is achieved via the restricted-unrestricted approach without introducing spin contamination into the evaluation of HFCCs. As expected, the results of such calculations are in line with the traditional unrestricted approaches for organic radicals, but show superior performance in case of HFCC in transition metal complexes.

On purely theoretical grounds, it is not very obvious which of the modern density functionals is the most appropriate to use in calculation of HFCCs.[22,25] The choice of a functional is strongly influenced by its reported performance in the study of different chemical systems. In general, generalized gradient approximation (GGA) functionals depending also on the kinetic energy density (meta-GGA) lead usually to no improvements over the GGA approximation,[30] and hybrid functionals tend to yield the

best results for a wide variety of organic systems.[21,22] The most recommended functionals in the literature seem to be PB86, PBE0, and B3LYP.[21,22,25] It should also be noted that reproducing trends in HFCCs as functions of structural parameters is a much easier task than matching the absolute values with experimental data. Such correlations are often achieved with almost any number of functionals. An important exception to the rule is observed with transition metal compounds for which none of the current density functionals shows uniform performance.[22,28]

For systems with heavier p-block elements or transition metals, relativistic effects *i.e.* spin-orbit and scalar relativistic corrections need to be treated appropriately.[14,24,25] In principle, this can be done using either wave function or DFT methods. However, due to their extremely high computational cost, correlated relativistic wave function-based calculations are generally limited to systems with only few tens of atoms. Hence, the majority of the relativistic HFCC calculations are at present time done using DFT which, when effectively parallelized, is capable of treating systems consisting of hundreds of atoms.

A common feature of many HFCC calculations is also the neglect of effects arising from external sources such as solid matrices or solvents. The external environment can, of course, have a major influence on the electronic structures of molecules. These effects can be approximated in calculations either explicitly, by modelling the whole unit cell or including a sufficient number of solvent molecules in the calculation, or implicitly, by using periodic boundary conditions or self-consistent reaction field methods.[24a]

2.3   Results and discussion

The following sections review the most important results described in the original research Papers **I–IV**. In the beginning of each section, a brief introduction to the current topic of main group radical chemistry is given.

2.3.1   Tetraimidophosphate dianion radicals

Polyimido anions of the p-block elements have in the recent years been of topical interest in main group chemistry in view of their versatile ligand behaviour and the novel cluster structures they form with alkali metals.[31] They are analogous to the more

common oxoanions such as $[CO_3]^{2-}$, $[SO_3]^{2-}$, and $[PO_4]^{3-}$ as the imido group $[NR]^{2-}$ is isoelectronic with the oxo $[O]^{2-}$ substituent. Thus, either by full (y = x) or partial (y < x) replacement of the oxo ligands in $[EO_x]^{z-}$ by imido groups, it has been possible to synthesize new classes of polyanions of the general type $[O_{x-y}E(NR)_y]^{z-}$ (E = p-block element), the chemical and physical properties of which differ significantly from those of their parent oxoanions, and depend on the ratio of imido:oxo units as well as on the size of the imido substituents.

Second only to silicon, phosphorus forms the largest number of oxoanions, many of which are of significant industrial importance.[32] It is therefore not surprising that numerous imido-analogues of phosphorus oxoanions have been prepared, including the trisimidometaphosphate $[P(NR)_3]^-$,[33] bisimidophosphinate $[R_2P(NR)_2]^{2-}$,[34] and the tetraimidophosphate $[P(NR)_4]^{3-}$ anions.[35] The only example of a tetraimidophosphate anion was for a number of years the naphthyl (Naph) derivative which was isolated as a solvent-separated ion pair $[Li(THF)_4]\{(THF)_2Li[(\mu\text{-NNaph})_2P(\mu\text{-NNaph})_2]Li(THF)_2\}$ from the curious reaction between P_2I_4 and Li_2NNaph.[35a] However, a recently published synthetic route involving the trilithiation of iminophosphoranes $Me_3SiN=P(NHR)_3$ provides a rational synthesis of the unsymmetrical tetraimidophosphates $Li_3[P(NR)_3(NSiMe_3)]$ (**1**) which exist in the solid state as centrosymmetric dimers containing a bicapped Li_6N_6 hexagonal prism.[35b]

$$2\ Me_3SiN=P(NHR)_3\ +\ 6\ n\text{-BuLi} \xrightarrow[-6\ n\text{-BuH}]{}$$

1
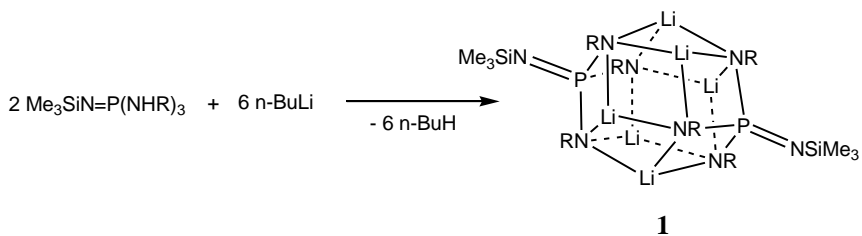
The discovery of the aforementioned simple synthetic route for **1** greatly facilitated investigations of the previously unexplored chemistry of these multidentate trianions. During the course of research it was noted that the initially colourless THF solutions of **1** became deep blue upon exposure to oxygen.[35b] This is reminiscent of the behaviour observed for the chalcogen centered polyimido anions in $\{Li_2[E(N^tBu_3)]\}_2$ (E = S, Se) which form deeply coloured persistent radicals upon oxidation.[36] After the initial observation, the one-electron oxidation of **1** (R = ^tBu) was attempted with an

equivalent amount of bromine or iodine. This resulted in a successful isolation of the stable neutral radicals {[Me$_3$SiNP(μ_3-N^{t}Bu)$_3$][μ_3-Li(THF)]$_3$X}$^\bullet$ (X = Br, I) (**2**).[37] In the solid state, the radical complexes adopt a distorted cubic structure in which a dilithiated tetraimidophosphate radical {Li$_2$[P(N^{t}Bu)$_3$(NSiMe$_3$)]}$^\bullet$ traps a monomeric LiX unit. Recently it was shown that this radical can also trap a monomeric lithium alkoxide, LiO^{t}Bu, forming a cluster {[Me$_3$SiNP(μ_3-N^{t}Bu)$_3$][μ_3-Li(THF)]$_3$O^{t}Bu}$^\bullet$ which is isostructural to **2**.[38]
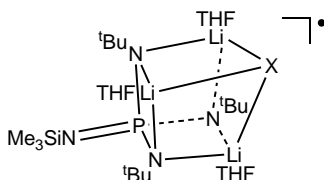
2

Initial spectroscopic studies of the radicals **2** (X = Br, I) in THF solution indicated that their EPR spectra are heavily dependent on concentration.[37] At high concentrations, the spectra contain components which suggest that a radical species with an approximate C_3 symmetry is present *i.e.* the cubic structure observed in the solid state is retained in solution. At extreme dilution, distortions in the EPR spectra were observed which were suggested to arise from the dissociation of the cubic framework to a monocyclic radical {[(Me$_3$SiN)(^{t}BuN)P(μ-N^{t}Bu)$_2$]Li(THF)$_2$}$^\bullet$, a THF solvated lithium halide, and a THF solvated lithium cation. This hypothesis was supported by isolating (THF)$_3$LiI from a solution of the iodide derivative; the limiting EPR spectrum of one such solution was also simulated with reasonable accuracy assuming it to be a monolithium species.

An interesting contrast to these observations is provided by the results from the investigations on the O^{t}Bu$^-$ derivative of **2**:[38] initial studies indicated that, excluding line broadening effects, its room temperature EPR spectrum is independent of sample concentration which suggests that no dissociation takes place. However, a satisfactory – though not perfect – spectral simulation was obtained by assuming that the cubic radical dissociates and forms the same monocyclic radical as obtained for the halide

derivatives. The THF solvated LiO^{t}Bu, the expected by-product of this solvation process, was not isolated from the solution.

The discovery of the stable cubic radicals **2** provides another illustrative example of the different chemistry the polyimido anions of the p-block elements undergo compared to that of the isoelectronic oxoanions: the phosphate radical $\{[PO_4]^{2-}\}^\bullet$ is a transient chemical species which is generally observed only in low temperature matrices.[39] At present time, these phosphorous-containing radicals are by far the most stable of their kind; they are also the only ones whose molecular structures have been unambiguously determined by X-ray crystallography (X = I, O^{t}Bu).[40] In light of these appealing characteristics, a more detailed study of the radicals incorporating a tetraimidophosphate dianion is a worthwhile endeavour in many aspects. The results of this study have been published in full length in Papers **I–II**.

Stable cubic radicals

To shed more light on the solution behaviour of the cubic radicals **2**, the one-electron oxidation of **1** (R = ^{t}Bu) was attempted with an equivalent amount of sulphuryl chloride (for a full description of experimental work conducted, see Paper **I**). This reaction yields a bright blue powder as an end product, the composition of which was assumed to be the neutral radical $\{[Me_3SiNP(\mu_3\text{-}N^tBu)_3][\mu_3\text{-}Li(THF)]_3Cl\}^\bullet$. Its EPR spectra were recorded as a function of concentration and temperature in THF solution; altering these variables was found to affect only the spectral linewidth and no distortions in signal positions were observed. In addition, the fine structure in the EPR spectrum showed little resemblance to the previously characterized derivatives of **2**, thereby excluding the possibility that the chloride derivative forms a radical species which is identical to the monocyclic species thought to have been observed earlier (X = Br, I, O^{t}Bu). Equally revealing were the results from DFT studies which indicated that the HFCCs calculated for the proposed monocyclic radical $\{[(Me_3SiN)(^tBuN)P(\mu\text{-}N^tBu)_2]Li(THF)_2\}^\bullet$ were significantly different from those gleaned from the experimental EPR spectra of O^{t}Bu$^-$ and I$^-$ derivatives of **2**. These results prompted a careful re-examination of the EPR data available for radicals **2** (X = Cl, Br, I, O^{t}Bu); DFT calculations probing the various possible structures for the radicals were also performed.

Spectral simulations employing the calculated HFCCs indicated that the computational results for the radicals in their solid state geometries are most effective at reproducing the general shape of the experimental spectra. A further refinement of these calculated HFCCs using a combination of spectral interpretation and iterative techniques yielded excellent simulations of the EPR spectra of both chloride and tert-butoxide derivatives of **2**. The experimental spectrum and its simulation are shown in Figure 2.1 for the Cl⁻ derivative; the spectrum is essentially a doublet due to a large coupling to ^{31}P 24.68 G (calculated value −28.6 G) which is further split to heptets by the three equivalent ^{14}N nuclei 5.26 G (3.2 G). The fine structure arises from smaller couplings to three ^{7}Li centres 2.19 G (−2.5 G), the fourth ^{14}N atom 0.40 G (−0.6 G), and the lone $^{35,37}Cl$ nucleus 0.10 / 0.08 G (0.20 / 0.17 G). The details of the simulations and calculations, as well as numerical values for the O^{t}Bu⁻ derivative are presented in full length in Paper **I**.
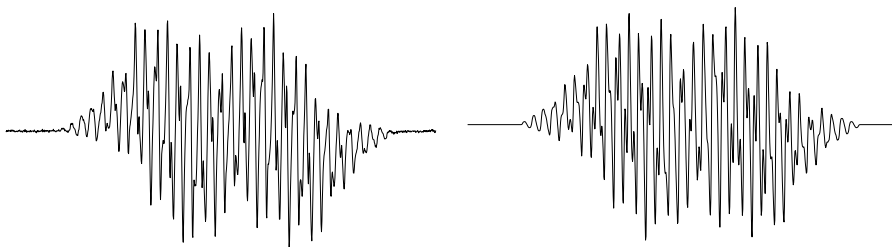

Figure 2.1 Experimental (left) and simulated (right) EPR spectra of the cubic radical {[Me$_3$SiNP(μ_3-N^{t}Bu)$_3$][μ_3-Li(THF)]$_3$Cl}$^{\bullet}$.

The HFCCs used in the spectral simulations of O^{t}Bu⁻ and Cl⁻ derivatives of **2** imply the presence of a molecule with C_3 symmetry; the numerical values are also in good agreement with results from calculations utilizing cubic geometries (see Paper **I**). Taken together, these findings clearly demonstrate that the O^{t}Bu⁻ and Cl⁻ derivatives retain their cubic structures in THF solution at all concentrations. This is consistent with the fact that the expected by-products of solvation, LiCl or LiO^{t}Bu, were never isolated. The HFCCs used in the simulations are essentially identical which further confirms that the Cl⁻ derivate of **2** is isostructural to the crystallographically characterized O^{t}Bu⁻ derivative. However, because the Li−X interaction is expected to change markedly

between the O^{t}Bu$^-$ and Cl$^-$ derivatives,[xi] so does the hyperfine coupling to the three magnetically active ^{7}Li nuclei. This effect, along with the different relative abundances and nuclear *g*-values of the magnetically active isotopes of O and Cl, is sufficient to produce the visible differences in the spectral fine structures (see Paper **I**).

In contrast to the results obtained for the O^{t}Bu$^-$ and Cl$^-$ derivatives, it proved impossible to simulate the limiting EPR spectra of both bromide and iodide derivatives with excellent accuracy by assuming retention of the cubic framework. However, good simulations of their EPR spectra were obtained using HFCCs that are similar to those present in Cl$^-$ and O^{t}Bu$^-$ derivatives, which indicates that the *major components* present in the THF solution are the cubic radicals {[Me$_3$SiNP(μ_3-N^{t}Bu)$_3$][μ_3-Li(THF)$_3$]Br}$^•$ and {[Me$_3$SiNP(μ_3-N^{t}Bu)$_3$][μ_3-Li(THF)]$_3$I}$^•$ (see Paper **I** for further details of simulation attempts).

The fact that the dissociation of the cubic structure at extreme dilution occurs for the bromide and iodide derivatives, but not for the chloride and tert-butoxide can be attributed to the weaker nature of the Li−X interactions when X = Br, I as compared to X = Cl, O^{t}Bu.[xi] In spite of countless attempts, the identities of the minor components present in the THF solutions of the bromide and iodide radicals could not be established unambiguously (see Paper **I**). However, the formation of crystalline (THF)$_3$LiI in low concentration solutions of the iodide derivative implies that the initial dissociation product in both cases is most likely the radical {[Li$_2$][P(NSiMe$_3$)(N^{t}Bu)$_3$]}$^•$ which is believed to adopt a spirocyclic geometry in THF solution, {(THF)$_2$Li[(μ-NSiMe$_3$)(μ-N^{t}Bu)P(μ-N^{t}Bu)$_2$]Li(THF)$_2$}$^•$ (*vide infra*).
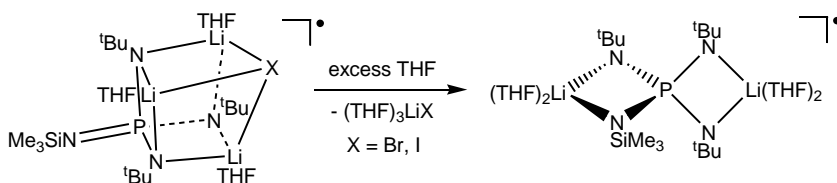
The stability of the cubic radicals **2** is thought to arise from primarily two factors: kinetic stabilization provided by the bulky ^{t}Bu groups and efficient delocalization of the

---

[xi] The mean Li−X bond lengths in the experimental structures of O^{t}Bu$^-$ and I$^-$ derivatives of **2** are 1.91 Å and 2.75 Å, respectively.[37,38] The calculated mean Li−X bond lengths for the Cl$^-$ and Br$^-$ derivatives are 2.34 Å and 2.49 Å, respectively.

unpaired electron to the three tert-butylimido nitrogen atoms. The latter was confirmed by examining the singly occupied molecular orbitals (SOMOs)[xii] of radicals **2**; the SOMOs of all derivatives are essentially identical and are composed of *p*-orbitals on the three nitrogen atoms within the cubic framework (see Figure 2.2). The effect of the identity of the imido substituents to the stability of the cubic tetraimidophosphate dianion radicals was studied in detail experimentally (for a full account, see Paper **I**). The replacement of ^{t}Bu groups to the sterically less demanding cyclohexyl substituents resulted in pronounced decrease in stability; all attempts to record EPR spectra of these transient radicals were unsuccessful as they persist only seconds in solution. In light of this result, the effect of replacing the ^{t}Bu groups to the sterically more encumbering adamantyl (Ad) cages was also tested. Rather expectedly, this structural alteration leads to the generation of stable radicals, the resulting EPR spectra of which are consistent with an approximately C_3 symmetric cubic structure (see Paper **I** for details). In addition, these EPR spectra are independent of concentration and temperature, irrespective of what oxidizing agent is used. Thus, the steric protection given by the adamantyl groups not only provides more kinetic stabilization by effectively hiding the unpaired electron from the surrounding medium, but also effectively prevents the disruption of the [μ_3-Li(THF)$_3$]X fragment by excess THF molecules.
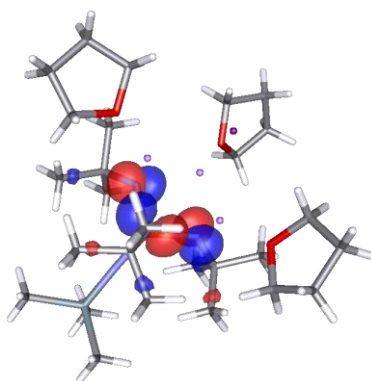
Figure 2.2 The SOMO of {[Me$_3$SiNP(μ_3-N^{t}Bu)$_3$][μ_3-Li(THF)]$_3$I}${}^{\bullet}$ displayed using isosurface values ±0.05.

[xii] Strictly speaking, the orbitals discussed in the text are in fact Kohn-Sham orbitals and not Hartree-Fock orbitals. Therefore, the abbreviation SOMO, although it is common practice, is in this instance sloppy quantum chemist's jargon.

Persistent spirocyclic radicals

During the investigations of the chemistry of polyimido anions of phosphorus, a rational synthetic route leading also to the *symmetric* tetraimidophosphates $Li_3[P(NR)_4]$ was devised and the R = ^tBu derivative was synthesized in good yield (see Paper **I**). Although X-ray quality crystals of this product could not be grown, its solution structure was determined by nuclear magnetic resonance (NMR) studies: like the known naphthyl derivative,[35a] the tetraimidophosphate anion $[P(N^tBu)_4]^{3-}$ adopts a spirocyclic conformation in THF and exists as the solvent-separated ion pair $[Li(THF)_4]\{(THF)_2Li[(\mu-N^tBu)_2P(\mu-N^tBu)_2]Li(THF)_2\}$. Thus, it was of interest to look into the chemistry of this species and, in particular, determine whether it would form highly stable radicals upon oxidation with halogens. The results of these investigations are presented in Paper **I**.
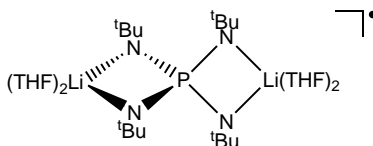
3

Rather than producing a cubic radical analogous to **2**, the one-electron oxidation of $[Li(THF)_4]\{(THF)_2Li[(\mu-N^tBu)_2P(\mu-N^tBu)_2]Li(THF)_2\}$ with halogens is expected to eliminate lithium halide and yield the neutral spirocyclic radical $\{(THF)_2Li[(\mu-N^tBu)_2P(\mu-N^tBu)_2]Li(THF)_2\}^\bullet$ (**3**). Quite unexpectedly, the formed radicals are persistent in nature and survive only a few days in THF; in the solid state their paramagnetic nature vanishes within minutes. The room temperature EPR spectra obtained from both iodine and sulphuryl chloride oxidations are identical, indicating that the halogen nucleus either has no spin density or, more likely, is not incorporated into the radical structure. An excellent simulation of the spectrum is obtained by including hyperfine couplings to one phosphorus atom, four equivalent nitrogen centres, and two lithium nuclei; the numerical values of the HFCCs used in the simulation are in good agreement with those given by DFT calculations assuming spirocyclic geometry (see Paper **I** for details). These results are consistent with the formation of the neutral

radical **3**, and suggest that the unpaired electron in it is delocalized equally over the four imido nitrogen atoms. The calculated SOMO of **3** is shown in Figure 2.3.
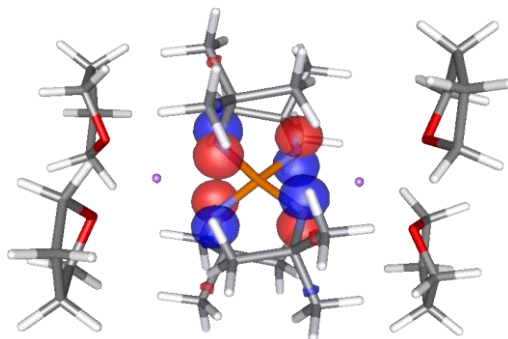

Figure 2.3 The SOMO of $\{(THF)_2Li[(\mu\text{-}N^tBu)_2P(\mu\text{-}N^tBu)_2]Li(THF)_2\}^\bullet$ displayed using isosurface values ±0.05.

The EPR spectrum of **3** is independent of sample concentration, indicating that the spirocyclic structure is retained even at extreme dilution. This is expected as both lithium cations in **3** are bis-chelated by two highly basic nitrogen atoms. Thus, it seems improbable that the instability of **3** compared to **2** is due to the strength of Li−N interactions. In addition, results from DFT calculations show that the energy gaps between the highest occupied (HO) and lowest unoccupied (LU) MOs in radicals **2** and **3** are not very different. Since the unpaired electron is more delocalized in the symmetric spirocyclic structure than in the cubic framework, this should, in principle, lead to *increased* stabilization in the former systems. The drastic drop in stability from the cubic radicals **2** to the spirocycle **3** must therefore result from the difference between the geometries of these species.

A comparison of space filling models for the two structures (excluding coordinated solvent molecules) suggests that the reactive nitrogen centres carrying most of the spin density are more accessible in the spirocycle than they are in the cubic framework. In this respect, it would be interesting to synthesize spirocyclic radicals analogous to **3** incorporating bulky imido substituents such as Ad, as their stabilities would indicate to which extent the geometry of the tetraimidophosphate radical **3** truly effects its lifetime. Also, characterization of the species present in solutions of **2** and **3** after they become diamagnetic would provide important insight to the mechanism by which these novel radicals lose their paramagnetic nature. Multinuclear NMR studies

have indicated that in case of the cubic radicals **2** this occurs presumably via dimerization.[37] Therefore, it is not unfounded to propose that it might also be the case for the spirocyclic radical **3**, the dimerization of which could readily occur through formation of Li−N ladder structures similar to the ones observed *e.g.* in the diamagnetic dimer $\{Li[P(N^tBu)(NH^tBu)_2(NSiMe_3)]\}_2$.[38]

Whilst exploring the reactions of the iminophosphoranes $RN=P(NHR')_3$ towards other metal alkyl reagents than n-butyllithium, it became obvious that $ZnMe_2$, $AlMe_3$, or $MgBu_2$ could not enforce a threefold deprotonation (see Paper **II**). In consequence, tetraimidophosphate radicals analogous to **2** and **3** in which all lithium cations would be replaced with other metals could not be synthesized, thereby preventing direct investigations of the effect of counterions on the radical stability.

A threefold deprotonation was, however, achieved with a stepwise approach in which the iminophosphoranes $RN=P(NHR')_3$ are treated *first* with one equivalent of $AlMe_3$ and, subsequently, with two equivalents of n-butyllithium (see Paper **II**). In the case of R = $SiMe_3$; R' = ^tBu derivative, this approach leads to the formation of the solvent-separated ion pair $[Li(THF)_4]\{Me_2Al[(\mu-NSiMe_3)(\mu-N^tBu)P(\mu-N^tBu)_2]Li(THF)_2\}$ which was characterized by NMR spectroscopy. Interestingly, when R = R' = ^tBu, the rather curious THF adduct $\{Me_2Al[(\mu-N^tBu)_2P(\mu_2-N^tBu)_2][\mu_2-Li(THF)]_2THF\}$ is crystallized; a single resonance in its ^7Li NMR spectrum confirms that formation of a solvent-separated ion pair does not occur even in excess THF.
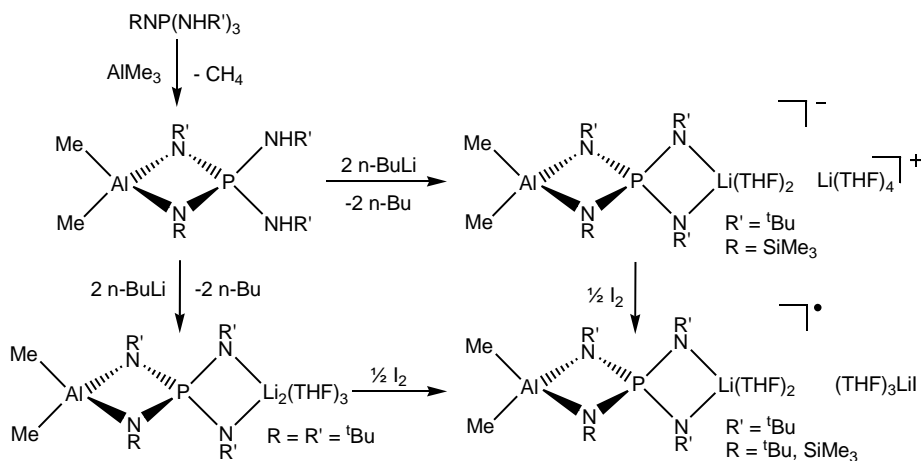
4

Preliminary experiments with these heterobimetallic tetraimidophosphates showed that when exposed to air, their THF solutions turn a bright blue colour indicative of the formation of radicals. Considering the initial geometries of these systems, their one-electron oxidations are expected to yield the neutral spirocyclic radicals $\{Me_2Al[(\mu-NR)(\mu-N^tBu)P(\mu-N^tBu)_2]Li(THF)_2\}^{\bullet}$ (**4**) (R = ^tBu, $SiMe_3$). Thus, the oxidation reactions were repeated using a stoichiometric amount of oxidizing agent (sulphuryl chloride, bromine, or iodine), and the resulting radicals were characterized by EPR spectroscopy; the results of these studies are presented in their entirety in Paper **II**.

Under standard conditions, the radicals **4** lose their paramagnetic nature within a couple of hours (solution) or minutes (solid state), and are thus considerably less stable species than **3**. However, both derivatives of **4** are sufficiently stable for EPR spectroscopic studies; they yield EPR spectra which show a primarily doublet pattern (due to the hyperfine coupling of approximately 30 G to ^{31}P nuclei) with a considerable amount of fine structure (see Paper **II**). To aid in the interpretation of these complex spectra, DFT calculations were performed for the spirocyclic model systems in which the bulky ^tBu and $SiMe_3$ substituents where replaced with Me and SiH_3 groups, respectively; the calculations suggested the presence of two equivalent ^{14}N couplings of around 6−7 G as well as a set of smaller HFCCs to the remaining ^{27}Al, ^7Li, and ^{14}N nuclei. Spectral simulations based on computational estimates reproduced the experimental EPR spectra of **4** with near-perfect accuracy (for full details, see Paper **II**) confirming the retention of spirocyclic structures upon oxidation.
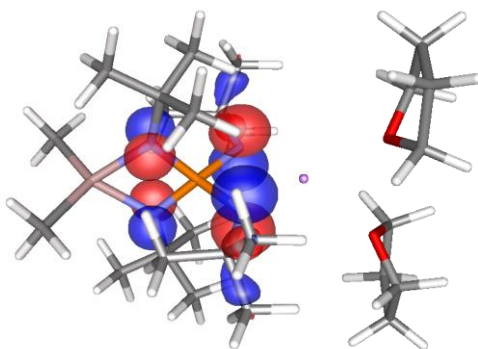

Figure 2.4 The SOMO of $\{Me_2Al[(\mu-N^tBu)_2P(\mu-^tBu)_2]Li(THF)_2\}^{\bullet}$ displayed using isosurface values ±0.05.

The results of the DFT calculations also showed that, due to the different fragment orbital energies of Li and $AlMe_2$, the SOMOs of radicals **4** are localized over the PNLiN ring (see Figure 2.4) and that the two imido nitrogen atoms in these rings carry more than 90% of the total spin density. The localization of the unpaired electron over two rather than four nitrogen centres rationalizes the lesser stability of **4** compared to **3** as it is expected to significantly facilitate dimerization through Li−N interactions. In this respect, the synthesis and characterization of the symmetric spirocyclic radical $\{Me_2Al[(\mu\text{-}N^tBu)_2P(\mu\text{-}N^tBu)_2]AlMe_2\}^\bullet$ having no lithium cations would be revealing.

## 2.3.2   Boraamidinato radicals

The monoanionic amidinates (**5**) are four-electron, bis-chelating donor ligands which have become important reagents in organometallic chemistry. They readily form complexes with numerous main group elements, transition metals, lanthanoids, and actinoids, all of which have been studied extensively;[41] recent studies have revealed that the prepared aluminium,[42,43] gallium,[43] and early transition metal complexes[44] of **5** function as catalysts for alkene polymerization.

5   **6**
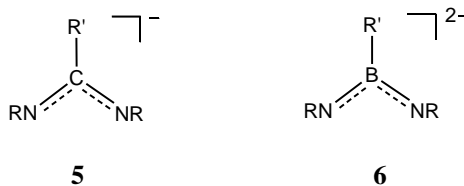
By contrast, the boraamidinate dianions (**6**) which are isoelectronic to the amidinates have received restricted attention. The known complexes of **6** were for a long time limited almost exclusively to elements from groups 4, 14, or 16, mainly due to a lack of versatile synthetic methodologies.[45] Recently, a new synthetic route leading to alkyl or aryl boraamidinates of the general formula $\{Li_2[R'B(NR)_2]\}_x$ (**7**) was discovered.[46] The extent of aggregation *i.e.* subscript x in the structural formula depends on the steric bulk of the substituents R and R': dimeric structures are observed in all cases except when R' = Me and R = ^tBu, or when R' = Ph and R = Dipp = 2,6-diisopropylphenyl, which form trimeric and monomeric complexes, respectively.

The synthesis of **7** involves the reaction of trisaminoboranes $B(NHR)_3$ with three equivalents of organolithium reagent R'Li which, besides effecting dilithiation, serves

as a nucleophile in the displacement of NHR group by the substituent R'. The dilithiated derivatives can be used in subsequent metathetical reactions, thus providing the most versatile route to complexes incorporating boraamidinate ligands.

$$3 \text{ LiR'} + \text{B(NHR)}_3 \longrightarrow 1/x \text{ \{Li}_2\text{[R'B(NR)}_2\text{]\}}_x + \text{LiNHR} + 2 \text{ R'H}$$

7
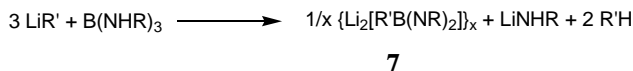
In view of current interest in the catalytic activity of aluminium and gallium amidinates, a detailed investigation of boraamidinate complexes with group 13 elements was recently conducted.[47] An intriguing observation in these studies was the formation of intensely coloured solutions when the boraamidinate reagents **7** were added to group 13 element halides MX_3 (M = B, Al, Ga, In) and the resulting reaction mixture was exposed to air; persistent bright pink solutions were also formed when reagents **7** were exposed directly to air.[48] The presence of radicals was confirmed using EPR spectroscopy. In both cases, the paramagnetic nature of the solutions was thought to be due to the formation of novel anion radicals of the type $\{\text{[R'B(NR)}_2\text{]}^-\}^\bullet$; analogous radical formation has not been observed for the amidinate ligands. These findings provided impetus to a more detailed study aiming to stabilize the paramagnetic systems via coordination to metal centres. The preliminary results of this study have been published in Paper **III**.

Spirocyclic group 13 complexes

Treatment of one equivalent of the dimeric dilithiated boraamidinate **7** (R' = Ph, R = ^{t}Bu) with one equivalent of metal halides MCl_3 (M = Al, Ga, In) in diethyl ether results in the formation of stable spirocyclic anions $[\text{PhB}(\mu\text{-N}^t\text{Bu})_2\text{M}(\mu\text{-N}^t\text{Bu})_2\text{BPh}]^-$ in low (< 30%) yields.[47,xiii] In the solid state, the anions chelate an ether solvated lithium cation via two nitrogen atoms (**8**) as evidenced by their X-ray crystal structures; in solution, the lithium cation exchanges rapidly on the NMR timescale between coordination to different pairs of N^{t}Bu nitrogen atoms.

[xiii] The reaction with $AlCl_3$ is in fact a two-step procedure in which *half* an equivalent of the dimeric boraamidinate **7** is first reacted with $AlCl_3$ producing the complex $[\text{PhB(N}^t\text{Bu})_2][\text{AlCl(OEt}_2)]$. The resulting complex can be isolated, crystallized, and reacted with another half an equivalent of **7**, thereby producing the desired product **8**.

$$\{Li_2[PhB(N^tBu)_2]\}_2 + MCl_3 \longrightarrow$$

8
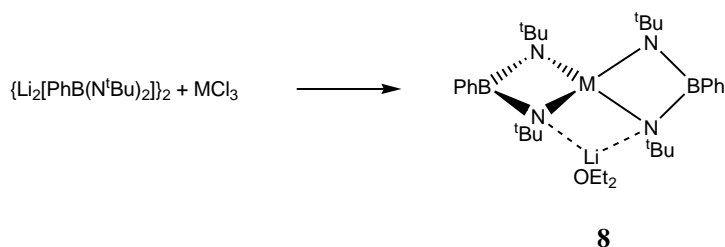
Subsequent reactions of **8** with half an equivalent of iodine generate dark red (M = Al), dark green (M = Ga), and green (M = In) solutions which persist from several days (M = Al) to only few minutes (M = In) at room temperature. These oxidation reactions are expected to eliminate lithium iodide and yield the neutral spirocyclic radicals [PhB(μ-N^{t}Bu)$_2$M(μ-N^{t}Bu)$_2$BPh]$^\bullet$ (**9**).

9
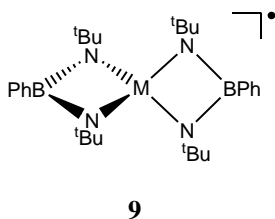
The EPR spectra of radicals **9** in diethyl ether solutions were recorded in room temperature and were found to be extremely rich in detail due to the hyperfine coupling of the unpaired electron to the nitrogen, boron, and metal atoms; the spectra are further complicated by the presence of two magnetically active isotopes of boron (^{10,11}B), gallium (^{69,71}Ga), and indium (^{113,115}In). To aid in the interpretation of these complex spectra, DFT calculations were performed for the spirocyclic model radicals [PhB(μ-NMe)$_2$M(μ-NMe)$_2$BPh]$^\bullet$ (M = Al, Ga, In) and the corresponding diamagnetic anions [PhB(μ-NMe)$_2$M(μ-NMe)$_2$BPh]$^-$ (see Paper **III** for full details).

Theoretical calculations revealed that the HOMO of the diamagnetic anions [PhB(μ-NMe)$_2$M(μ-NMe)$_2$BPh]$^-$ transforms as the a_2 irreducible representation in the D_{2d} point group (see Paper **III**). Thus, a one-electron oxidation of **8** is expected to yield neutral radicals **9** with $^2A_2$ ground state, D_{2d} symmetry, and uniform spin delocalization throughout the two boraamidinate ligands (*cf.* the oxidation of structurally related group 13 diazabutadiene spirocycles for which the HOMO is doubly degenerate[49]). The

25

calculated SOMO of the M = Ga derivative of **9,** depicted in Figure 2.5, shows the expected characteristics.
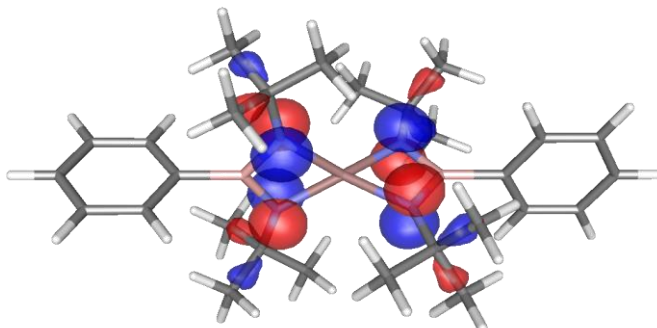
Figure 2.5 The SOMO of [PhB(μ-N^{t}Bu)$_2$Ga(μ-N^{t}Bu)$_2$BPh]$^\bullet$ displayed using isosurface values ±0.05.

The HFCCs yielded by the DFT calculations were used in simulations as initial estimates of the true couplings present in radicals **9**; excellent simulations of the spectra of aluminium and gallium derivatives were obtained upon further optimization of these values (see Paper **III**). The EPR spectrum of the indium derivative clearly shows the presence of at least two radicals of which the major component − the dectet of multiplets − is unmistakably identified as the spirocyclic radical [PhB(μ-N^{t}Bu)$_2$In(μ-N^{t}Bu)$_2$BPh]$^\bullet$ (see the EPR spectrum and its simulation in Figure 2.6).[50] Hence, the simulations and DFT calculations confirm that the iodine oxidation of **8** produces the expected spirocyclic radicals **9** which exhibit uniform spin delocalization throughout the two boraamidinate ligands.

Figure 2.6 Experimental (left) and simulated (right) EPR spectra of [PhB(μ-N^{t}Bu)$_2$In(μ-N^{t}Bu)$_2$BPh]$^\bullet$.

Crystals grown from the concentrated diethyl ether solutions of **9** (M = Al, Ga) are stable under inert atmosphere at room temperature for weeks, thus enabling X-ray crystal structure determinations. The analyses confirmed that the two complexes are isostructural and exist in the delocalized spirocyclic geometries also in the solid state (see Paper **III**).
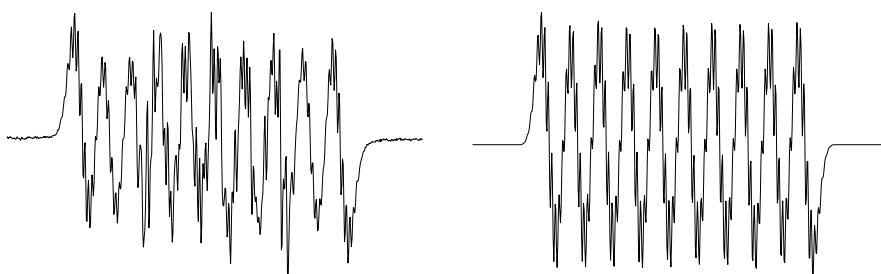
The room temperature EPR spectrum of [PhB(μ-N^{t}Bu)$_2$In(μ-N^{t}Bu)$_2$BPh]$^•$ was monitored as a function of time, and was observed to undergo significant changes over the course of only few minutes: a rapid decrease in the signal intensity assigned to the spirocyclic component is accompanied by a simultaneous increase in the intensity of signals arising form other paramagnetic species.[50] A difference spectrum between the initial spectrum (Figure 2.6) and a spectrum measured after 10 minutes gives some indication of the identity of the emerging radicals (see Figure 2.7).
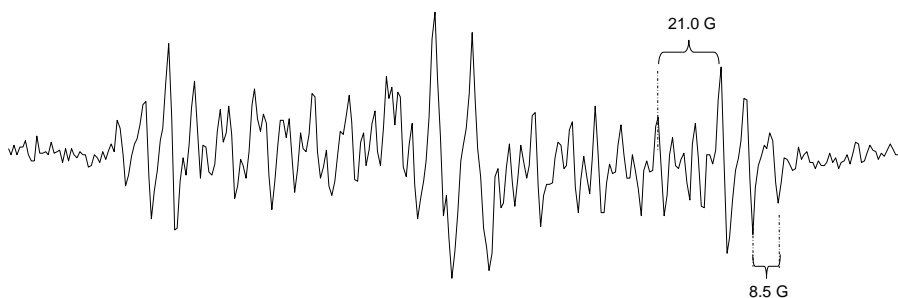
Figure 2.7 Experimental EPR spectra of [PhB(μ-N^{t}Bu)$_2$In(μ-N^{t}Bu)$_2$BPh]$^•$
after 10 minutes of oxidation.

The central high-intensity multiplet in Figure 2.7 is not symmetric with respect to the left- and right-hand sides of the spectrum. Hence, at least two different radicals give rise to the EPR signal in Figure 2.7. The outer ends of the spectrum display a 34 G wide pentet pattern suggesting the presence of an 8.5 G hyperfine coupling to two equivalent nitrogen nuclei. Upon closer inspection, this pattern is found to be repeated ten times within the spectrum which is consistent with the presence of approximately 21 G coupling to a single ^{115}In atom, a spin-9/2 nucleus. Interestingly, no clear indication of a significant (> 1.5 G) coupling to a boron nucleus is seen. It is tempting to assign this radical as the monocycle [PhB(μ-N^{t}Bu)$_2$In]$^•$. Such an assignment is, however, highly unlikely as the monocycle is expected to be an indium centered radical and should

therefore display a [115]In HFCC which is several orders of magnitude larger than the observed coupling.

As more time passes, the dectet pattern slowly vanishes and the central multiplet begins to dominate the EPR spectrum of [PhB(μ-N^{t}Bu)$_2$In(μ-N^{t}Bu)$_2$BPh]$^\bullet$. Before disappearing completely, this multiplet evolves into a simple three line pattern displaying an approximately 13 G hyperfine coupling to one nitrogen atom. It is clear that further experimental studies are needed before the identity of the unknown components present in the EPR spectrum of [PhB(μ-N^{t}Bu)$_2$In(μ-N^{t}Bu)$_2$BPh]$^\bullet$ can be established with certainty. In this respect, it might be instructive to try to oxidize the analogous indium spirocycles incorporating sterically encumbering imido substituents[46b] as they could provide greater kinetic stabilization and, thus, slow the reactivity of the radical and the resultant transformations observed in its EPR spectrum.

Lastly, the synthesis of the boron-containing analogue of **8** was attempted by treating the dilithiated boraamidinate Li$_2$[PhB(N^{t}Bu)$_2$] with BF$_3$ in a 2:1 molar ratio.[50] Colourless crystals were isolated from the resulting bright purple solution; a subsequent single-crystal X-ray analysis revealed that, instead of the expected spirocyclic complex [Li(OEt$_2$)][PhB(μ-N^{t}Bu)$_2$B(μ-N^{t}Bu)$_2$BPh], the crystals contained an asymmetrically substituted borazine.[51] However, multinuclear NMR data from the coloured reaction mixture indicated that the desired spirocyclic complex most likely exists in the solution; further studies have shown that there exists two competing reaction pathways, one of which gives the borazine and the other produces the spirocyclic complex. Hence, the reaction mixture was exposed to oxygen, after which its EPR spectrum was recorded; the resulting spectrum and its simulation are presented in Figure 2.8.

DFT calculations done for the model system [PhB(μ-NMe)$_2$B(μ-NMe)$_2$BPh]$^\bullet$ indicated that, if the radical species giving the EPR spectrum in Figure 2.8 is the expected spirocycle, hyperfine couplings of similar magnitude to the central (-8.43 G for [11]B) and outer (-6.64 G for [11]B) boron nuclei, as well as to the four equivalent nitrogen atoms (4.59 G) should be observed.[50] The corresponding values used in the simulation are 6.92 G and 5.56 G for the central and outer [11]B nuclei, respectively, and 5.46 G for the equivalent nitrogen centres. Hence, the spectral simulations and the calculated HFCCs provide solid evidence for the assignment of the paramagnetic species as the spirocyclic radical [PhB(μ-N^{t}Bu)$_2$B(μ-N^{t}Bu)$_2$BPh]$^\bullet$.
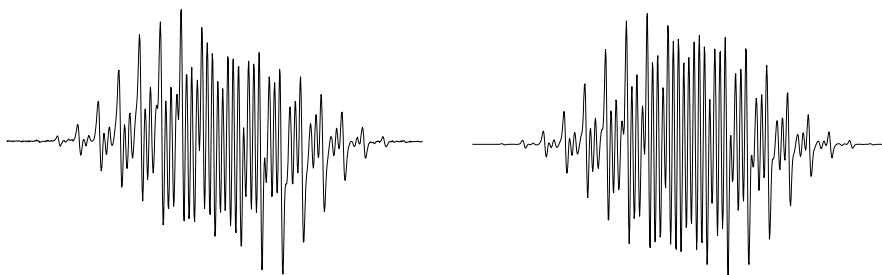
Figure 2.8 Experimental (left) and simulated (right) EPR spectra of
$[PhB(\mu\text{-}N^tBu)_2B(\mu\text{-}N^tBu)_2BPh]^{\bullet}$.

Although crystals of the paramagnetic boron spirocycle $[PhB(\mu\text{-}N^tBu)_2B(\mu\text{-}N^tBu)_2BPh]^{\bullet}$ suitable for X-ray crystallography could not be grown, the radical appears to be highly stable in diethyl ether. In fact, it showed no indication of decomposition over a period of weeks; solutions stored for years at low temperatures (5°C) were also found to give highly intense EPR signals.[50]

In summary, the neutral radicals **9** are the first examples of complexes in which the boraamidinate anion radicals "$\{[PhB(N^tBu)_2]^-\}^{\bullet}$" are stabilized by coordination to metal centres. The successful isolation and characterization of these paramagnetic systems demonstrates that the redox behaviour of boraamidinates contrasts the well-established chemistry of the isoelectronic amidinate systems, and is a much more important feature than heretofore recognized.

Monocyclic lithium complex

After the successful characterization of the spirocyclic group 13 boraamidinate complexes, the identity of the radicals present in the air oxidized solutions of systems **7** $\{Li_2[R'B(NR)_2]\}_2$ was reinvestigated.[50] To this end, the complex $\{Li_2[PhB(N^tBu)_2]\}_2$ was oxidized with an equivalent amount of iodine.

The oxidation reaction produced bright pink solutions which were found to be transient at room temperature. Hence, the paramagnetic solutions were cooled to −80°C immediately after the oxidation and subjected to a variable-temperature EPR study. The resulting low temperature (−60°C) EPR spectrum is depicted in Figure 2.9.[50]
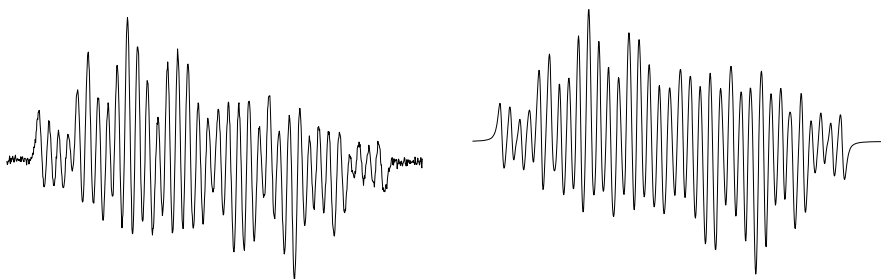
Figure 2.9 Experimental (left) and simulated (right) EPR spectra of $[PhB(\mu\text{-}N^tBu)_2Li(OEt_2)_x]^{\bullet}$.

The spectrum shows a distinct pentet pattern due to the coupling of the unpaired electron to two equivalent nitrogen atoms; the measured hyperfine coupling constant is 8.51 G. An equally distinctive feature is the repetitive quartet pattern with a HFCC of 2.14 G which is tentatively assigned to the coupling of the unpaired electron to single ^7Li nucleus. Perhaps a bit more obscure is the quartet pattern with a coupling of 11.18 G which creates the spectral width; this coupling is assigned to the ^{11}B nucleus. A spectral simulation based on these HFCCs was found to reproduce the experimental EPR spectrum with excellent accuracy (see Figure 2.9). Hence, the experimental information indicates that the observed radical is the monocyclic species $[PhB(\mu\text{-}N^tBu)_2Li(OEt_2)_x]^{\bullet}$ (**10**). Subsequent DFT calculations yielded HFCCs that are in good agreement with the values gleaned from the experimental spectrum which further supports this assignment.
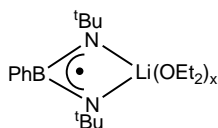
10

Increasing the sample temperature to $-10°C$ resulted in the disappearance of the hyperfine coupling to the lithium nucleus, which was immediately followed by a complete loss of an EPR signal via a transient five line spectrum. This strongly suggests that the monocyclic radical is either decomposing by losing a lithium cation or dimerizing though Li−N interactions. In the light of results obtained for the tetraimidophosphate radicals (*vide supra*), the latter scenario seems to be the more plausible alternative.

2.3.3 1,4-diaza-1,3-butadienide radicals

During the past quarter of a century, 1,4-diaza-1,3-butadiene (DAB) ligands (**11**) have attracted considerable attention as useful reagents in organometallic chemistry due to their coordination and redox properties. The lone pairs of the nitrogen atoms and the π-electrons of the C=N bonds allow these molecules to act as electron donors, which allows coordination to metals using 2, 4, 6, or 8 electrons. The DAB ligands not only coordinate metals as neutral molecules, but also as anions or dianions by accepting one or two electrons from the metal, respectively. In addition, the identities of the four substituents on the N=C–C=N backbone can be varied, allowing for the steric and electronic properties of the ligand to be fine-tuned; the ligand substituted at the nitrogen atoms with the ^{t}Bu group (R = ^{t}Bu-DAB, R' = H) has been widely employed in research.

$$
\begin{array}{cc}
\underset{RN}{\overset{R'}{\underset{\|}{C}}}\!\!-\!\!\underset{NR}{\overset{R'}{\underset{\|}{C}}} & \underset{RN\ \ominus\ NR}{\overset{R'}{C}=\overset{R'}{C}}
\end{array}
$$

11   **12**
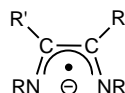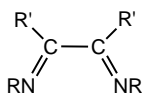
At present, DAB ligands have been coordinated to several transition metal elements,[52] to lanthanoids such as europium and gadolinium,[53] as well as to a range of main group elements including silicon[54] and germanium.[55] A number of the synthesized metal complexes are catalytically active and can affect a broad spectrum of chemical reactions.[56] In recent years, a growing interest in complexes of the DAB ligand which contain group 13 elements has emerged and many novel systems have arisen from this work.[57] Of especial importance have been the anionic species [(R-DAB)M:]$^-$ (M = Al, Ga)[58] which are isoelectronic with the stable N-heterocyclic Arduengo-type carbenes [(R-DAB)C:].[59]

More closely aligned with the present thesis are the known group 13 metal complexes which formally contain the DAB ligand as a monoanion radical (**12**), formed from the one-electron reduction of the parent species **11**. Several different types of paramagnetic DAB complexes incorporating the heavier group 13 elements have recently been characterized.[60] However, despite the wealth of X-ray structural data available for them, significantly less is known of their electronic structures and, especially, their spin density distributions. Although the reported *g*-values imply that all

know complexes are primarily ligand centred π-radicals, the fine structures in their EPR spectra are poorly resolved due to the coupling of the unpaired electron to a number of magnetically active nuclei. In consequence, it is difficult to extract accurate values of the HFCCs and, thus, the spin densities, from these spectra. In many cases, this has led to spectral assignments that are tentative at best.[60]
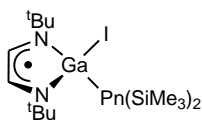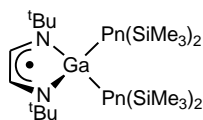
13   **14**

Recently, the isolation and structural characterization of the monocyclic paramagnetic complexes {(^{t}Bu-DAB)Ga[I][Pn(SiMe$_3$)$_2$]}$^\bullet$ (**13**) (Pn = N, P, As) and the related dipnictogen species {(^{t}Bu-DAB)Ga[Pn(SiMe$_3$)$_2$]$_2$}$^\bullet$ (**14**) (Pn = P, As) were reported.[60h] The EPR spectra of these novel radicals proved to be quite complex and accurate simulations were not achieved due to "slight differences in ^{69,71}Ga hyperfine couplings and isotropic *g*-values". However, the electronic Zeeman interaction does not depend on nuclear isotopes and the HFCCs of ^{69}Ga and ^{71}Ga isotopes are, according to Equation (2.6), inter-related by the ratio of their nuclear *g*-factors provided that the EPR spectra show no significant anisotropies. Despite the above shortcomings in the interpretation, the magnitudes of the hyperfine interactions in **13** and **14** have been *estimated*;[60h] it is not entirely surprising that the reported values do not even reproduce the general shapes of the experimental spectra. In light of these facts, a DFT study of the complexes **13** and **14** was undertaken in order to determine their electronic structures, spin densities, and HFCCs, which together would give a more realistic picture of spin delocalization in such systems. The complex EPR spectra of these radicals were then re-interpreted in terms of the computationally predicted HFCCs. The results of such investigations are presented in their entirety in Paper **IV**.

Electronic structures

Due to the size of the systems in question, calculations for **13** and **14** were carried out using model systems in which the SiMe$_3$ groups attached to the pnictogen atoms were replaced with a computationally less demanding SiH$_3$ groups. As a whole, the calculated

geometries for the model systems are in good agreement with the crystallographically determined structures,[60h] taking into account the lesser steric effects of the SiH$_3$ groups compared to SiMe$_3$ (structural details are discussed more thoroughly in Paper **IV**). Thus, the HFCCs calculated utilizing the optimized geometries are also expected to be fairly close to the true values provided that the chosen functional-basis set combination provides a reasonable description of the spin densities at the magnetically active nuclei.

The SOMOs of **13** and **14** are essentially identical, as expected, seeing that they all are ligand centered radicals. In all instances, the SOMO is localized on the DAB ligand and is composed of nitrogen and carbon p-orbitals; it is bonding along the C−C bond and anti-bonding between the C−N linkages. The SOMOs have no s-contribution from the central metal or DAB hydrogen atoms, and only very small contributions from the pnictogen and halogen nuclei. The SOMO of the model system {(^{t}Bu-DAB)Ga[As(SiH$_3$)$_2$]$_2$}$^\bullet$ is depicted in Figure 2.10.
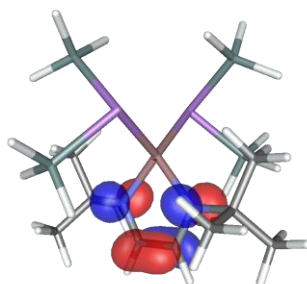
Figure 2.10 The SOMO of {(^{t}Bu-DAB)Ga[As(SiH$_3$)$_2$]$_2$}$^\bullet$
displayed using isosurface values ±0.05.

Hyperfine interactions

The HFCCs of the model systems {(^{t}Bu-DAB)Ga[I][Pn(SiH$_3$)$_2$]}$^\bullet$ (Pn = N, P, As) and {(^{t}Bu-DAB)Ga[Pn(SiH$_3$)$_2$]$_2$}$^\bullet$ (Pn = P, As) were calculated using both relativistic and non-relativistic methods, and only a brief summary of the results is given here. A full account of the theoretical methods employed as well as complete listings of the numerical values of HFCCs can be found in Paper **IV**.

The calculated values of the ^{1}H, ^{14}N, and ^{69,71}Ga HFCCs in radicals **13** and **14** show only minor variation throughout the systems. The predicted ^{1}H and ^{14}N HFCCs are approximately 6 G and 5 G, respectively. These values are consistent with the

hyperfine couplings observed in other related DAB centered radicals,[61] but deviate significantly from the estimated values.[60h] Although the SOMOs have no *s*-contribution from gallium, the calculated ^{69,71}Ga couplings of 15−30 G arise from a combination of spin polarization effects and relatively high nuclear *g*-values of the two isotopes of gallium. Only small HFCCs are calculated to the pnictogen atoms in **13**: 0.5 G, 6.4 G, and 3.5 G for N, P, and As, respectively. These couplings vary roughly with the relative magnitudes of the nuclear *g*-values of ^{14}N, ^{31}P, and ^{75}As nuclei, which implies of a nearly constant spin density on the pnictogen centres. A significant ($\approx$ 17 G) hyperfine interaction to the ^{127}I nuclei is also calculated for radicals **13**; in contrast, the HFCC to iodine was assumed to be negligible in the published analyses.[60h] The dipnictogen complexes **14** show equal hyperfine couplings to the two group 15 atoms of the PnSiH$_3$ substituents; the couplings are minute (1 G) for the nitrogen species, but significantly larger for both phosphorus (9 G) and arsenic (5 G) radicals.

Excellent simulations of the experimental EPR spectra of all mono- and dipnictogen complexes were obtained using the calculated HFCCs as initial estimates of the true couplings, and optimizing the sets of values using a combination of iterative methods and spectral interpretation. The experimental and simulated EPR spectra of {(^{t}Bu-DAB)Ga[I][N(SiMe$_3$)$_2$]}$^\bullet$ are illustrated in Figure 2.11 as an example; the spectral simulations of other complexes are described in detail in Paper **IV**.
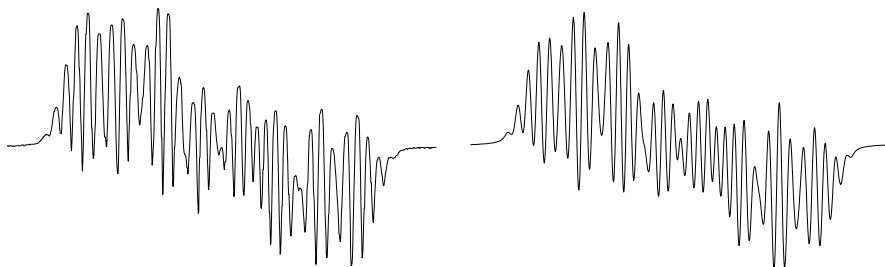
Figure 2.11 Experimental (left) and simulated (right) EPR spectra of {(^{t}Bu-DAB)Ga[I][N(SiMe$_3$)$_2$]}$^\bullet$.

As expected, the experimental EPR spectrum of {(^{t}Bu-DAB)Ga[I][N(SiMe$_3$)$_2$]}$^\bullet$ does not display a quartet pattern characteristic of a large coupling to gallium, a spin-3/2 nucleus. Instead, the spectrum shows a sextet pattern due to a large coupling to ^{127}I (spin-5/2) which dominates the spectrum. The slight differences between the left- and

right-hand sides of the experimental spectrum (*i.e.* the lack of perfect inversion symmetry with respect to peak intensities) are caused by small anisotropies as well as higher-order hyperfine interactions due to the presence of large HFCCs to the heavy nuclei ^{69,71}Ga and ^{127}I; a third-order perturbation theory-based Hamiltonian was utilized to accurately model the experimental spectrum.

The HFCCs used to create the simulation in Figure 2.11 are very close to the hyperfine couplings calculated for the model system; the same applies also to the other complexes **13** and **14** discussed herein. The errors in the calculated HFCCs for the second and third row nuclei are on the average 15−20% which is a fairly typical result for DFT calculations of π-radicals using hybrid functionals.[22] The deviations for the heavier nuclei are slightly larger. Nevertheless, the calculations predict the relative magnitudes of the HFCCs accurately and the numerical values are reasonably close to the true values so that the iterative spectral optimization process converges without much difficulty. Hence, the optimized HFCCs derived from the DFT calculations can be regarded as the actual HFCCs present in these systems.

Implications of the results

It is already obvious from above that the spectral analyses reported for complexes **13** and **14** are erroneous.[60h] However, it is informative to discuss them in more detail, as these results have implications for several other studies reported for related paramagnetic group 13 metal complexes of the DAB ligands.[60e−g,i]

In previous spectral analyses,[60h] the possibility for a significant iodine coupling in radicals {(^{t}Bu-DAB)Ga[I][Pn(SiMe$_3$)$_2$]}$^{\bullet}$ was ruled out based on results obtained for the closely related systems {(^{t}Bu-DAB)GaI$_2$}$^{\bullet}$,[60e] {(Dipp-DAB)GaI$_2$}$^{\bullet}$,[60i] and {(Dipp-DAB)AlI$_2$}$^{\bullet}$.[60e] For these species, experimental evidence − or rather lack thereof − has suggested that only minor (< 1 G) ^{127}I couplings are present. However, an alternative spectral interpretation of the poorly resolved EPR spectrum of {(^{t}Bu-DAB)GaI$_2$}$^{\bullet}$ has been presented which employs approximately 8 G HFCCs to iodine atoms.[60g] In addition, results from EPR studies on some valence isoelectronic zinc systems {[(^{t}Bu-DAB)ZnX$_2$]$^{-}$}$^{\bullet}$ (X = Cl, Br), the spectra of which are well-resolved, have demonstrated that the bromine derivative displays 9 G coupling to the ^{79,81}Br nuclei.[62] In light of these results and the computational data reported in Paper **IV**, it appears highly unlikely that

the group 13 systems $\{(R\text{-}DAB)MI_2\}^\bullet$ (M = Al, Ga) would display such small HFCCs to iodine as previously suggested. Recent computational studies on these systems support this conclusion and indicate that some of the radicals $\{(R\text{-}DAB)MX_2\}^\bullet$ which are characterized in solution by EPR and ENDOR spectroscopies are not the same radicals that were identified in the solid state by X-ray crystallography.[63] Further studies are, however, needed before the true identities of these species can be unambiguously determined.

Continuous wave ENDOR studies of the complexes **13** and **14** in frozen solutions have also been reported.[60h] These studies indicated only small hyperfine couplings of 3.795 MHz (approximately 1.5 G) to the ^{1}H nuclei on the DAB backbone. In a recent EPR study,[60i] such anomalously small HFCCs were concluded to arise from the electronic effects caused by the ^{t}Bu substituents on the DAB nitrogen atoms; this rationalization was also used to explain the EPR spectra of several other paramagnetic complexes of the ^{t}Bu-DAB ligand with group 13 metals.[60e] Such a claim is clearly refuted by the present computational results which show that the identity of the substituents on the nitrogen atoms has only a marginal effect on the ^{1}H HFCCs. Moreover, in the same study[60i] it was found that the identity of the substituents on the DAB backbone also influences the spin density on the gallium atom as extremely small (1–2 G) HFCCs to ^{69,71}Ga nuclei were found in both $\{(^t\text{Bu-DAB})GaI_2\}^\bullet$ and $\{[(^t\text{Bu-DAB})GaI]_2\}^{\bullet\bullet}$. In this respect, it is interesting to note that the gallium HFCCs determined in Paper **IV** for **13** and **14** are one of the *highest* reported for such systems. Other apparent inconsistencies in the reported experimental data also exist.

As demonstrated in this section, the extant EPR spectroscopic data for the paramagnetic group 13 metal complexes incorporating DAB ligands appears to pose more questions than answers.[60] The results reported in Paper **IV** show that, when combined with EPR simulation software, density functional calculations can provide a powerful tool for interpreting even very complex EPR spectra. Thus, the results described herein lend strong support that computational studies would also provide important insight into the electronic structures of other known group 13 DAB radicals; detailed theoretical investigations of these systems are currently being pursued.[63]

Chapter 3

Diradicals and diradicaloids

Diradicals are thought to play a pivotal role in bond breaking and formation; a large variety of thermal and photochemical reactions are generally believed to involve diradicals either as short-lived intermediates or transition states along the reaction coordinate.[64] While this has provided much of the motivation for the study of diradicals in the past, the driving force behind this research in the recent years has shifted towards studying diradicals as both theoretically and experimentally interesting species in their own right.

Diradicals can function as potential building blocks for materials with novel magnetic, optical, and conducting properties.[65] In addition, diradicals could be used in spin-based electronics, spintronics, provided that a practical method for controlling their spin states exists. The foremost goal in the ongoing work has therefore been to acquire a better theoretical understanding of the factors governing the spin interactions in diradicals. Such insight would allow the design of extended systems with a number of unpaired electrons, the interactions of which could be manipulated to produce desirable properties in bulk materials.

A major factor which hinders the research into diradicals is their relatively short lifetime under standard laboratory conditions.[64] This results from their bifunctionality which permits intermolecular as well as intramolecular coupling reactions. In general, triplet radicals are significantly more stable than their singlet counterparts, which is a

direct manifestation of the fact that most chemical reactions generally occur on singlet potential energy surfaces on which the latter systems do not usually represent energy minima. Thus, along with spin interactions, the factors affecting the stability of diradicals form the core of current diradical research. Efficient delocalization of the unpaired electrons and the use of bulky substituents to prevent coupling reactions are simple means of increasing the lifetimes of radicals (of any kind). Unfortunately, both of these methods tend to impede the potential applicability of diradicals in chemical applications as their exploitation isolates the radical centres from the surroundings.

Over the past decade, research advancements have brought stable singlet diradicals to the fore. In part, this is because triplet radicals, having longer lifetimes, have already become relatively well-understood species, whereas the most stable singlet diradicals known (*e.g.* 2,2-diethoxy-1,3-diphenylcyclopentane-1,3-diyl[66]) have lifetimes on the order of microseconds. However, the syntheses of several stable singlet diradicals with variable amounts of diradical character (diradicaloids) have recently been reported.[1] Their diminished reactivities do not fully suppress radical-type chemical behaviour; singlet diradicaloids can find potential applications as initiators for radical reactions and as radical scavengers.[67] Also, singlet diradicals are of particular interest to nonlinear optics research due to their unusually high second-order hyperpolarizabilities,[68] and as building blocks for antiferromagnetic low-spin polymers exhibiting metallic conductivity.[69]

The electronic structures and molecular properties of some main group singlet diradicaloids were discussed in Papers **V** and **VI**.

3.1   Definition and theoretical background

A diradical is a molecule in which two electrons occupy two different MOs, ϕ_A and ϕ_B, which have the same, or nearly the same, energy.[70] In a radical with one unpaired electron on one orbital, there are, in the absence of a magnetic field, two energetically degenerate configurations (Slater determinants); in one of the configurations the unpaired electron has α spin, in the other it has β spin. In a diradical, six electronic configurations become possible when two electrons are placed in two MOs (see Figure 3.1)

It is obvious that the configurations χ_1 and χ_2 are both singlets, and that χ_5 and χ_6 are the high-spin components of a triplet state. Less obvious is the fact that both χ_3 and χ_4 violate the principle of indistinguishability of identical particles *i.e.* the uncertainty principle, and neither of them alone is a pure spin eigenfunction representing either a singlet or a triplet state. However, the linear combination ($\chi_3 + \chi_4$) represents the third component of a triplet and the combination ($\chi_3 - \chi_4$) is a third siglet.
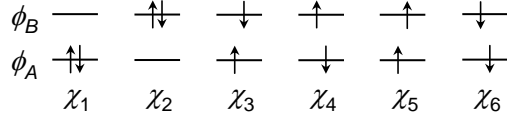
Figure 3.1 Configurations which can be generated by distributing two electrons in two MOs ϕ_A and ϕ_B.

Since there are three different singlet configurations, there are three possible singlet wave functions that can be formed from them.[70] If the two orbitals ϕ_A and ϕ_B have the same symmetry, so do the three configurations χ_1, χ_2, and ($\chi_3 - \chi_4$), and symmetry ensures that all of them contribute to each of the three different singlet states. If ϕ_A and ϕ_B belong to two different symmetry representations, as it is more often the case, ($\chi_3 - \chi_4$) has different symmetry from the totally symmetric configurations χ_1 and χ_2, and cannot therefore mix with them. In such case, ($\chi_3 - \chi_4$) represents one of the three possible singlet states and the orthogonal linear combinations ($\chi_1 + \chi_2$) and ($\chi_1 - \chi_2$) represent the two other possible alternatives. The resulting six wave functions, three singlets, Ψ^s, and three triplets, Ψ^s, are then composed as follows

$$\Psi_1^s = \tfrac{1}{\sqrt{2}}[\lambda(\phi_A)^2 - \sqrt{1-\lambda^2}\,(\phi_B)^2](\alpha\beta - \beta\alpha), \tag{3.1}$$

$$\Psi_2^s = \tfrac{1}{\sqrt{2}}[\lambda(\phi_A)^2 + \sqrt{1-\lambda^2}\,(\phi_B)^2](\alpha\beta - \beta\alpha), \tag{3.2}$$

$$\Psi_3^s = \tfrac{1}{2}(\phi_A\phi_B + \phi_B\phi_A)(\alpha\beta - \beta\alpha), \tag{3.3}$$

$$\Psi_1^t = \tfrac{1}{2}(\phi_A\phi_B - \phi_B\phi_A)(\alpha\beta + \beta\alpha), \tag{3.4}$$

$$\Psi_2^t = \tfrac{1}{\sqrt{2}}(\phi_A\phi_B - \phi_B\phi_A)(\alpha\alpha), \tag{3.5}$$

$$\Psi_3^t = \tfrac{1}{\sqrt{2}}(\phi_A\phi_B - \phi_B\phi_A)(\beta\beta). \tag{3.6}$$

In accordance with the Pauli exclusion principle, the spatial components of the singlets are symmetric and the spin parts are antisymmetric. The opposite is true for the triplet states. In systems where MOs ϕ_A and ϕ_B are degenerate by symmetry, configurations χ_1 and χ_2 appear in the linear combinations with equal weights, $\lambda = 2^{-\frac{1}{2}}$. If the orbital degeneracy is lifted by a reduction in symmetry, the configurations χ_1 and χ_2 enter the wave functions with different coefficients, $2^{-\frac{1}{2}} < \lambda < 1$. The former systems are often referred to as *pure* singlet diradicals, whereas for the latter, non-degenerate, case the term singlet *diradicaloid* is used.

The presence of four possible states, a triplet and three singlets, inevitably raises the question of which one is the ground state.[70] For diradicaloids, two cases need to be considered. If λ is close to 1, the non-degeneracy of the orbitals ϕ_A and ϕ_B generally ensures a singlet ground state. For intermediate values of λ, the singlet state falls below the triplet if the difference in one-electron energy of ϕ_A and that of ϕ_B is significantly greater than the exchange integral between these two MOs. For pure diradicals the question is more subtle. The molecular analogue of Hund's rule predicts that when one electron is placed in each of two different MOs, the triplet state will lie below the singlet in energy.[71] If the two MOs ϕ_A and ϕ_B have exactly the same energy, the lowest energy singlet wave function can always be written as having one electron in each of two MOs – either ϕ_A and ϕ_B, or a linear combination thereof.[xiv] Therefore, Hund's rule predicts that pure diradicals should always have a triplet ground state.

Hund's rule is an embodiment of the Pauli exclusion principle which forbids two electrons of same spin to simultaneously appearing in the same region of space. However, two electrons of opposite spins are not subject to the exclusion principle and can be located in the same region of space at the same instant of time. In consequence, two same spin electrons typically have a lower mutual electron-electron repulsion energy compared to the two opposite spin electrons which occupy the same pair of MOs, ϕ_A and ϕ_B. Although the aforementioned rule holds for the majority of cases, an exception to it arises if the two MOs are disjoint *i.e.* have no atoms in common. The two electrons occupying the orbitals, one each, will then never appear in the same region of

---

[xiv] This is trivial for $\Psi^s{}_3$. The linear combination $\Psi^s{}_1$ is always lower in energy than $\Psi^s{}_2$ and can easily be rearranged to a form $\Psi^s{}_1 = N\,[\phi_X\phi_Y + \phi_Y\phi_X]\,(\alpha\beta - \beta\alpha)$, where $\phi_X = \phi_A + \phi_B$, $\phi_Y = \phi_A - \phi_B$, and N is an appropriate normalization constant.

space be their spins parallel or anti-parallel. Thus, the triplet state is no longer energetically favoured over the singlet and both states should have nearly the same energy. In such diradicals, Hund's rule can be violated and, consequently, the singlet state may fall below the triplet in energy.

A mathematical justification for the above reasoning can be formulated by considering the explicit energy expressions of the three singlet states and one triplet state.[70] Since the orbitals ϕ_A and ϕ_B are degenerate, the one-electron operators in the Hamiltonian (kinetic energy and nuclear-electron attraction) give the same energy for each of the four states, and the relative energy ordering of the different states is then completely determined by the two-electron operator describing the electron-electron repulsion. The resulting relative energies, expressed in terms of Coulomb (J) and exchange (K) integrals, are

$$E(\Psi_1^s) = \tfrac{1}{2}(J_{AA} + J_{BB}) - K_{AB} = J_{AA} - K_{AB}, \tag{3.7}$$

$$E(\Psi_2^s) = \tfrac{1}{2}(J_{AA} + J_{BB}) + K_{AB} = J_{AA} + K_{AB}, \tag{3.8}$$

$$E(\Psi_3^s) = J_{AB} + K_{AB}, \tag{3.9}$$

$$E(\Psi_{1-3}^t) = J_{AB} - K_{AB}, \tag{3.10}$$

where $J_{AA} = J_{BB}$ is the Coulomb repulsion energy between two electrons in the same MO (the equality follows from the degeneracy of the orbitals ϕ_A and ϕ_B), J_{AB} is the Coulomb repulsion energy between two electrons in different degenerate MOs, and K_{AB} is the quantum mechanical exchange correction to the Coulomb repulsion energy. K_{AB} equals the Coulomb repulsion between two electrons, for each of which the probability distribution is given by the product $\phi_A\phi_B$.[xv]

The Coulomb repulsion integral between two electrons in the same MO is always greater than that between electrons in different orbitals: $J_{AA} > J_{AB}$.[70] Consequently, Equations (3.7)–(3.10) lead directly to Hund's rule and predict a triplet ground state for any diradical in which the partially occupied orbitals are degenerate. The reduction in electron-electron repulsion energy due to the Pauli exclusion principle is also visible in the equations: for the triplet state subtraction of K_{AB} from the Coulomb repulsion energy

---

[xv] In reality, the same MOs ϕ_A and ϕ_B are never optimal for all four states and the values of the parameters J_{AA}, J_{BB}, J_{AB}, and K_{AB} in Equations (3.7)–(3.10) are likely to be somewhat different.

computed for uncorrelated electrons, J_{AB}, corrects for the fact that electrons are correlated and tend to avoid each other.[xvi] Moreover, for disjoint diradicals, the exchange integral K_{AB} becomes very small and the energy of a singlet state approaches that of a triplet. In such cases, the electron-electron interactions between the two electrons in the partially filled MOs and the electrons in the other lower lying orbitals can lead to selective stabilization of the singlet state and, ultimately, to a violation of Hund's rule.

3.2   Quantum chemical methods

It is evident from above that all three singlet wave functions in Equations (3.1)–(3.6) are of two-configuration form. The Hartree-Fock wave function, be it restricted or unrestricted, is therefore by nature a qualitatively incorrect approximation of the wave functions Ψ^s_{1-3} and should not be used to describe singlet diradical states of molecules.[24] The use of an UHF wave function in this purpose has, however, sometimes been justified by noting that it includes some of the static electron correlation effects by allowing α and β MOs to localize to different atomic centres.[72] Although this reasoning is theoretically correct, it is only half the truth. An analysis of a UHF wave function for a singlet state shows that it is not a pure spin state but instead a spin contaminated mixture of singlet and triplet states (*vide supra*). Although it behaves qualitatively correctly in some cases *e.g.* it ensures correct molecular dissociation, it should not constitute the basis of any quantitative analysis of singlet diradicals. However, the existence of a symmetry-broken singlet UHF wave function that is lower in energy than the corresponding RHF wave function can be used as a *qualitative* indicator of a diradical character. This subject is closely related to the concept of wave function stability.

In an SCF calculation, the variational procedure ensures that all converged solutions are stationary points on the energy hypersurface.[24] However, this does not guarantee that the solutions correspond to either local or global energy minima. To

---

[xvi] Electron correlation in the singlet state Ψ^s_1 follows from the fact that the wave function for this state can be written in an alternate form (see Footnote xiv) which assigns one electron in an orbital of the form ($\phi_A + \phi_B$) and an electron, of opposite spin, in an orbital of the form ($\phi_A - \phi_B$). Consequently, the two electrons reside in spatially different orbitals, which reduces the Coulomb repulsion energy by K_{AB}.

ensure that a solution is a true minimum, the second derivatives of the energy with respect to all orbital coefficients should also be calculated. Alternatively the stability of a SCF solution can also be tested with respect to constraint of orbital double occupancy (only RHF), real *vs.* complex-valued MOs, and orbital symmetry. If all resulting eigenvalues are positive, the solution is a true energy minimum with respect to given perturbations. A negative eigenvalue indicates instability whose nature and effect to the wave function should subsequently be characterized. In many cases, RHF-UHF instability indicates the presence of singlet diradical character.

Although the triplet wave function in Equation (3.4) is also of two-configuration form, the corresponding high-spin components in Equations (3.5) and (3.6) are not. Thus, these states can be accurately described by any single-reference method, the accuracy of the approach being increased as one proceeds from a simple Hartree-Fock wave function to the highly correlated CI or CC wave functions.[24,72] Because all three triplet wave functions Ψ^t_{1-3} give the same energy[xvii], it is accustomary to use either (3.5) or (3.6) in calculations. Thus, calculations for triplet states of diradicals are conceptually much simpler than calculations for the corresponding singlet states. One should, however, bear in mind that the use of an UHF wave function as a zero-order approximation re-introduces the problem of spin contamination, because UHF wave functions for triplet states are also contaminated by states of higher multiplicities. There are two solutions to this problem: the contributions from the unwanted states can be removed by applying appropriate projection operators, or a ROHF wave function, which is a true eigenfunction of the spin operator, can be used as a zero-order wave function.

Contrary to the triplet case, the theoretical first-principles treatment of singlet diradicals is a challenging quantum chemical task and only multiconfigurational models capable of treating the major configurations on an equal footing provide a qualitatively correct zero-order wave function.[24,72,xviii,73] Although Equations (3.1)–(3.3) suggest that a two-configuration wave function is sufficient, a balanced description of electron correlation effects requires the use of multiconfigurational wave functions with much

---

[xvii] This is naturally true only in the absence of an external magnetic field and if one neglects the, usually minute, effect of zero-field splitting to the energy.

[xviii] By virtue of the infinite-order feature of the coupled cluster and quadratic configuration interaction methods, they also have the ability to handle moderate amounts of static electron correlation. Recently, several formally single-reference-based methods capable of describing multiconfigurational wave functions have also been presented.[73]

larger active orbital spaces. The greatest difficulty, common to all multiconfigurational methods, then becomes selecting the configurations that need to be included in the zero-order wave function. Typically either complete active space (CAS) or restricted active space (RAS) SCF methods are used. However, even these methods have an intrinsic level or arbitrariness as the MOs included in the active space must be chosen manually. The best choice is naturally to employ the full valence space which ensures that the MCSCF wave function becomes flexible enough to describe all major interactions between valence electrons. This is, however, only possible for small molecules as both CAS and RAS calculations become unmanageably large for active spaces encompassing more than 16 orbitals. Hence, the choice of an active space is usually guided by physical considerations which change from system to another.

For quantitative accuracy, the chosen multiconfigurational wave function needs to be augmented by dynamic correlation; in general, MCSCF methods perform equally well, or poorly, for diradicals as RHF does for molecules with closed-shell singlet ground states.[24,72] The inclusion of dynamic electron correlation can be done using configuration interaction, perturbation theory, or coupled cluster-based approaches. If computationally feasible, configuration interaction methods (MRCI) are preferable as they give energies which are variationally bound. Perturbation theory-based methods provide good alternatives that are non-variational but computationally much less demanding.

Up to this point density functional theory has not been discussed within the context of diradicals. The next paragraphs will approach this topic from two viewpoints: first assuming that the exact exchange-correlation functional $E_{xc}[\rho]$ is known, and, second, considering the performance of current $E_{xc}[\rho]$ functionals. As seen below, the two boundary conditions lead to very different results. Therefore, it is of utmost importance to always specify whether DFT is discussed in an exact or approximate sense.

The Kohn-Sham DFT method applied so frequently in quantum chemistry is nothing more than a particular rearrangement of the Hohenberg-Kohn theorems and leads to the exact energy of the electronic Schrödinger equation in all situations provided that the exact exchange-correlation functional $E_{xc}[\rho]$ is known.[25] Although the Kohn-Sham formalism has the look and feel of a single-determinant method with its

shortcomings, it is an essentially *exact* method even for systems such as singlet diradicals for which multiconfigurational wave functions need to be used.[xix] For example, an exact potential curve for the dissociation of H_2 can be obtained using a single-determinant Kohn-Sham reference system provided that the exact $E_{xc}[\rho]$ is used.[74] In addition, the effective potential used in the Kohn-Sham equations has no reference to spin which suggests that the all-decisive variable in every case is the total electron density *i.e.* the sum of α and β densities. Thus, the Kohn-Sham formalism is equally suitable for any kind of molecule, be it open or closed-shell, again, provided that the exact exchange-correlation functional $E_{xc}[\rho]$ is known.

Unfortunately, none of the modern day approximate $E_{xc}[\rho]$ functionals comes even sufficiently close to the exact functional for the above to be true in any practical applications.[25] For this reason, density functionals that depend explicitly on α and β densities are used, and restricted and unrestricted Kohn-Sham formalisms are constructed analogously to their Hartree-Fock counterparts.

Using the unrestricted Kohn-Sham formalism, DFT can be easily applied to study the triplet states of radicals.[25,72] However, an important limitation of approximate DFT is that it cannot be successfully applied, in its standard form, to the majority of systems for which the ground state wave function is multiconfigurational. This restriction includes also singlet diradicals. There are two exceptions to the rule. If the two partially occupied orbitals ϕ_A and ϕ_B are disjoint, the errors in unrestricted symmetry-broken DFT calculations tend to be very small.[75] Also, DFT calculations that use pure functionals (no exact exchange) generally show satisfactory performance for singlet diradicaloid systems provided that their diradical character is only moderate.[25] This is due to the fact that the description of static electron correlation effects is, at least to some extent, built-in to the density functionals. Given that both approaches push the limits of theory to extremes, the accuracy of the results should always be checked using experimental data or high-level wave function calculations as a reference.

The stability of a SCF solution was discussed earlier in the context of RHF. In principle, restricted-unrestricted instabilities found for Kohn-Sham solutions can be used in similar fashion to confirm the presence of singlet diradical character.[25] The

---

[xix] Only a handful of pathological cases for which a non-degenerate interacting ground state density cannot be represented by a single Slater determinant have been identified.

converse is, however, not true: the wave function can have an internal instability even if all eigenvalues in the Kohn-Sham SCF stability analysis are found to be positive. For RHF, the instability of the spin-restricted SCF solution is a direct indication of the quality of the zero-order wave function, whereas in the DFT framework of electronic structure theory, the instability mirrors the capability of the chosen exchange-correlation functional to describe the electron density with a single Slater determinant comprised of Kohn-Sham orbitals. Because most density functionals are capable of describing small amounts of singlet diradical character, the restricted Kohn-Sham method is much less prone to internal instabilities than RHF. For example, it is for this reason that the spin-restricted DFT solutions are stable for ozone whose singlet diradical character is determined to be approximately 26% by wave function methods.

This discussion is concluded by noting that although the symmetry-broken unrestricted formalism is commonly used to simulate the static electron correlation effects in DFT, more practical solutions to the multiconfigurational problem also exist. Most of these approaches to date have been hybrids of the conventional multiconfigurational treatments with the Kohn-Sham method.[76] Two other important alternatives exist: simulation of static electron correlation effects using fractionally occupied Kohn-Sham orbitals,[77] and expressing the density and energy of a strongly correlated system in terms of ensemble of densities and energies built from several single Kohn-Sham determinants.[78] As it is so common in quantum chemistry, each solution has its own drawbacks; however, a detailed discussion of these is not given here.

Specific issues related to the applicability of different theoretical methods in describing the electronic structures of diradicals were discussed in depth in Papers **V** and **VI**.

3.3   Singlet diradicaloids in main group chemistry

Singlet diradicals have fascinated chemists for decades because the synthesis of such species would pave the way for new developments in electric, magnetic, and optical applications. As discussed earlier, singlet diradicals are typically not energy minima on chemical reaction coordinates, but transient chemical species having lifetimes that are only fractions of a second. The primary research goal has therefore been to synthesize

singlet diradicaloids with lifetimes on the order of days or weeks, which still display a significant amount of radical character.
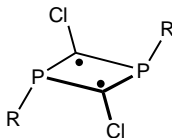

15

These efforts have not been in vain: in recent years, a number of stable main group singlet diradicaloids with variable amount of diradical character have been synthesized.[1,79] The major breakthrough was the synthesis of the 2,4-diphosphacyclobutane-1,3-diyls (**15**) which were the first diradicaloid species prepared in gram quantities.[1a] Shortly thereafter, they were followed by several other main group diradicaloids, all of which possess the same four-membered 22 valence electron ring motif that is present in **15**.[1b–d,xx,80] The following subsections give a brief review of the known systems.

3.3.1   Cyclobutane-1,3-diyl

An organic diradical which can be regarded as the parent species of all following inorganic diradicaloids is cyclobutane-1,3-diyl (**16**).
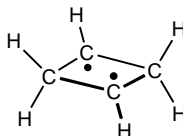

16

Although compound **16** itself has eluded synthesis, several 1,3-substituted structures have been prepared and spectroscopically characterized.[81] The lack of steric protection around the radical centres ensures that these are all extremely short-lived chemical species which can only be observed in low temperature matrices. EPR spectroscopic studies have further shown that all derivatives of **16** have triplet ground states; singlet cyclobutane-1,3-diyls are only predicted to be transition states for the ring inversion of

---

[xx] For the sake of completeness, it should be noted that examples of stable main group diradicaloids based on other structural motifs are also known *e.g.* pentastanna[1.1.1]propellanes. They are, however, not as abundant groups as the four-membered ring systems.[80]

bicyclobutane. An important question which immediately arises is whether structural modifications to the carbon-based four-membered ring motif in **16** could be used to stabilize the diradical and to alter its spin state.

3.3.2 Group 14 analogues of cyclobutane-1,3-diyl

Intuitively, the best candidates for the synthesis of inorganic singlet diradicals are the heavier group 14 analogues of cyclobutane-1,3-diyl (**17**), E = Si, Ge, Sn, and Pb.
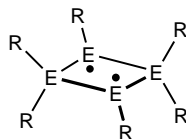

17

Quantum chemical calculations for the model systems (R = H) have demonstrated that the silicon and germanium species exhibit bond stretch isomerism *i.e.* have two distinct minima on the potential energy surface which mainly differ by the length of one transannular E–E interaction.[82] However, neither of the two energy minima corresponds to a fully planar structure like cyclobutane-1,3-diyl **16** which implies that transannular bonding interactions are considerably stronger in the heavier group 14 systems **17** than in **16**. In addition, only the bicyclic non-radical isomers which have short, classic, E–E bonds have been experimentally observed.[83] This is presumed to be due to the use of σ-donating groups in place of hydrogen atoms that were used in calculating the model diradicaloids which renders the bicyclic form energetically favourable. A particularly interesting case is the sterically crowded bicyclic silicon derivative (E = Si ; R = ^{t}Bu, 2,6-Et$_2$C$_6$H$_3$), the atypical chemical and physical behaviour of which reveals the close energetical proximity to the diradicaloid form.[83]

3.3.3 2,4-diphosphacyclobutane-1,3-diyls

As mentioned earlier, 2,4-diphosphacyclobutane-1,3-diyls **15** were the first singlet diradicaloid species isolated in gram quantities.[1a] They can be prepared by reacting two equivalents of C-dichlorophosphaalkene with one equivalent of n-butyllithium at 100°.
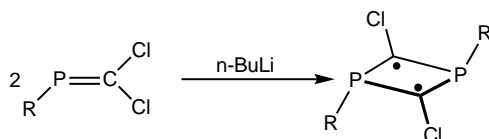
Alternatively, treatment of amino(dichloromethylene)phosphane $R_2NP=CCl_2$ with ^tBuLi under equivalent conditions leads to the analogous amino derivatives with $P-NR_2$ functionalities.[84] However, such species are thermally unstable at room temperature and isomerize rapidly both in solution and in the solid state.

The chloro substituents of **15** can be exchanged by the addition of *e.g.* HgR'_2 followed by treatment with n-BuLi and ^tBuOH.[85] This gives the asymmetric protonated derivatives (**18**).
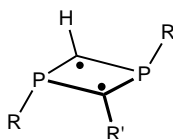
18

Compounds of type **18** can subsequently be deprotonated using lithium di(iso-propyl)amide to give unusual anionic carbenes, which further react with $AlMe_3$ to yield anionic diradicaloids (**19**),[86] or with R''Cl to produce the fully substituted diradicaloids (**20**).[87]
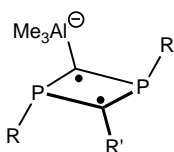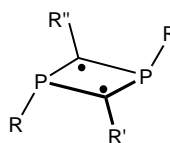
19   **20**

An alternate synthetic approach leading to almost quantitative amounts of 2,4-diphosphacyclobutane-1,3-diyl derivatives similar to **20** is to react phosphaalkynes, $R-C\equiv P$, with half an equivalent of tert-butyllithium, followed by quenching with alkyl halides such as iodomethane or benzyl chloride.[88]

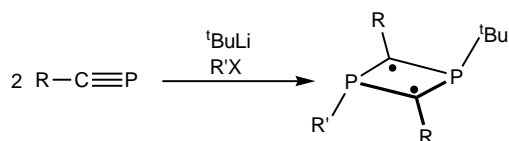The X-ray crystal structure of **15** where R = Mes* = 2,4,6-^{t}Bu$_3$C$_6$H$_2$ displays a planar P$_2$C$_2$ unit in which the substituents at the carbon atoms adopt a trans orientation to one another, as do the two groups bonded to the phosphorus atoms (See Figure 3.2).[1a] The carbon atoms are significantly less pyramidalized ($\sum\angle_C$ = 347.3°) than the phosphorus atoms ($\sum\angle_P$ = 337.9°) and show no significant transannular bonding interaction (the observed C–C distance is 2.43 Å). A planarization of all substituents, which would lead to cyclic π-conjugation, is not observed because of the relatively high inversion barrier of phosphorus.[1a] X-ray crystal structures of **18** (R = Mes* ; R' = SiMe$_3$)[85] and **20** (R = Mes* ; R' = Me ; R'' = ^{t}Bu)[88a] indicate that these also contain planar P$_2$C$_2$ units with the substituents attached to the phosphorus atoms displaying a trans configuration. However, the ring carbon atoms in these compounds are not pyramidalized but essentially planar ($\sum\angle_C$ = 358−360°) indicating stronger π-conjugation than in **15**.
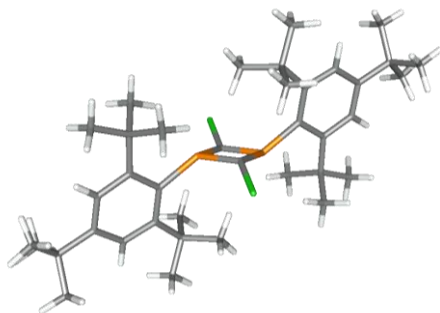
Figure 3.2 The X-ray crystal structure of **15** R = Mes*.[1a]

All reported 2,4-diphosphacyclobutane-1,3-diyls are EPR silent which indicates that they have singlet ground states. Although the planar ring form of (HP)$_2$(CH)$_2$ is calculated to be energetically less stable than the bicyclic structure with a transannular C–C bond, its isomerization to the bicyclic form via C–C bond formation is forbidden according to the Woodward-Hoffmann rules.[1a] Consequently, upon heating the 2,4-

diphosphacyclobutane-1,3-diyls do not isomerize via ring closure but by cleavage of the P–C bond.[1a, xxi,84]

3.3.4   1,3-dibora-2,4-diphosphoniocyclobutane-1,3-diyls

After the pioneering work involving the synthesis of 2,4-diphosphacyclobutane-1,3-diyls, several other inorganic analogues of cyclobutane-1,3-diyl have been prepared. The most controversial of these have been the 1,3-dibora-2,4-diphosphoniocyclobutane-1,3-diyls (**21**).[1b]
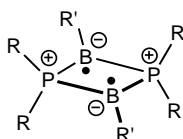
21

Given the appropriate substituents, these diradicaloids are stable both in solution and in the solid state.[1b] The synthesis of **21** proved to be simple: reaction of the 1,2-dichorodiborane with two equivalents of secondary lithium phosphide LiPR$_2$ at −80° give **21** as yellow, air sensitive, but thermally stable crystals in good yield.
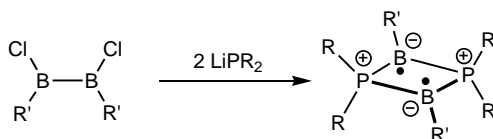
   The single-crystal X-ray analysis of **21** (R = ^{i}Pr ; R' = ^{t}Bu) shows a perfectly planar P$_2$B$_2$ ring (see Figure 3.3); the central carbon atoms of the ^{t}Bu substituents lie also in the four-membered ring plane.[1b] The transannular B–B distance is 2.57 Å which indicates that the B–B bond in 1,2-dichlorodiborane (1.68 Å when R' = 2,4,6-trimethylphenyl[89]) has indeed been cleaved.

---

xxi In contrast, the photolysis of some derivatives of **15** leads almost quantitatively to the bicyclic isomers.[84]
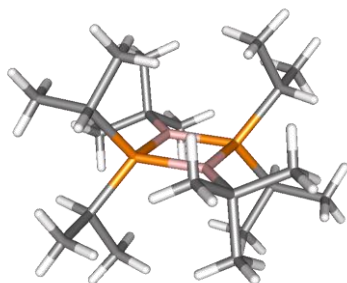
Figure 3.3 The X-ray crystal structure of **21** (R = ^{i}Pr ; R' = ^{t}Bu).[1b]

Quantum chemical calculations done for the model system $(H_2P)_2(BH)_2$ show that the planar structure is a transition state for the inversion of the bicyclic B–B σ-bonded isomer of **21**.[1b,90] Also, a thermal ring closure of $(H_2P)_2(BH)_2$ to the bicyclic form is symmetry-allowed; *cf.* $(HP)_2(CH)_2$. Thus, it is understandable that stabilization and isolation of **21** in its planar form is only possible using substituents which are sterically much more demanding than hydrogen; DFT calculations carried out for **21** (R = ^{i}Pr ; R' = ^{t}Bu) confirm the conformation observed from the X-ray data to be an energy minimum on the potential energy surface.[1b]

3.3.5   1,3-distanna-2,4-diazacyclobutane-1,3-diyls and 1,3-digerma-2,4-diazacyclobutane-1,3-diyls

The most recent inorganic diradicaloids formally derived from cyclobutane-1,3-diyl are the two heterocycles with heavier group 14 elements: 1,3-digerma-2,4-diazacyclobutane-1,3-diyl (**22**) (Ar = 2,6-Dipp$_2$C$_6$H$_3$)[1c] and 1,3-distanna-2,4-diazacyclobutane-1,3-diyl (**23**). [1d]

22   **23**
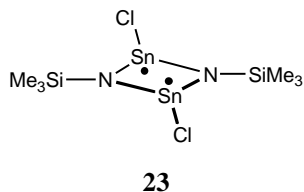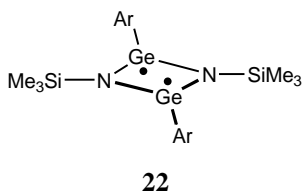
Diradicaloid **22** can be prepared by oxidizing digermyne with trimethylsilyl azide.[1c]

ArGeGeAr + 2 N$_3$SiMe$_3$ $\xrightarrow{-2 N_2}$

Me$_3$Si—N...Ge(Ar)...Ge(Ar)...N—SiMe$_3$
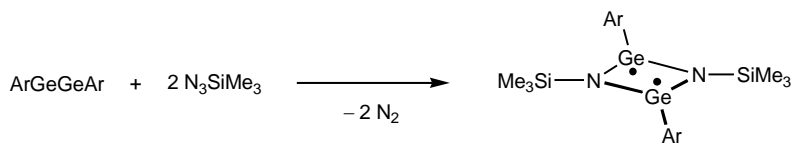
Compound **23** can be synthesized by the rather peculiar reaction of chloro(amino)stannylene dimer with AgOCN.[1d]

(Me$_3$Si)$_2$N—Sn(Cl)(Cl)Sn—N(SiMe$_3$)$_2$ $\xrightarrow[\substack{- C(NSiMe_3)_2 \\ - Ag / CO_2}]{AgOCN}$ Me$_3$Si—N...Sn(Cl)...Sn(Cl)...N—SiMe$_3$
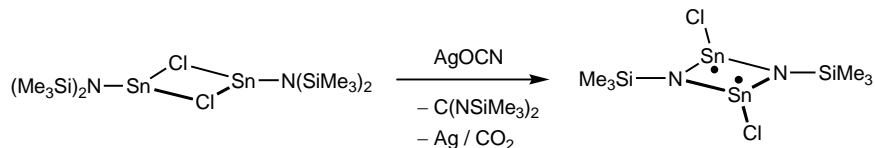
Both **22** and **23** have similar four-membered ring skeletons composed of two heavier group 14 elements and two nitrogen atoms, with the radical centres localized on the group 14 elements.[1c,d] Their X-ray crystal structures reveal perfectly planar four-membered rings in which both nitrogen atoms are trigonal planar, while the two group 14 atoms are pyramidal; the crystal structure of **23** is depicted in Figure 3.4. The two substituents attached to the group 14 atoms are in a trans configuration. The Sn−Sn distance in **23** is 3.40 Å and the corresponding Ge−Ge distance in **22** is 2.76 Å which are about 0.60 Å and 0.40 Å longer than typical Sn−Sn and Ge−Ge single bonds.
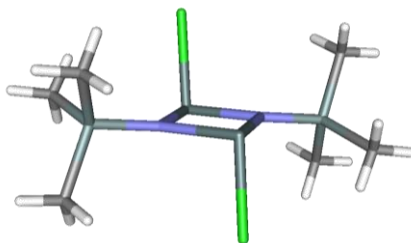
Figure 3.4 The X-ray crystal structure of **23**.[1d]

Diradicaloids **22** and **23** are diamagnetic both in the solid state and in solution. DFT calculations have shown that the singlet states of **22** and **23** are 60−70 kJ mol^{-1} more stable than the triplet.[1c,d] For both species, the symmetry of the highest occupied molecular orbital does not allow thermal isomerization to the bicyclic form via transannular bond formation.

3.3.6   Disulphur dinitride

Disulphur dinitride, S_2N_2 (**24**), is in many ways an intriguing chemical species. Its synthesis has been achieved via the thermal decomposition of S_4N_4 in the presence of silver wool.[91] Initially, the reaction of S_4N_4 vapour with silver gives silver(I)sulfide, Ag_2S, which subsequently catalyses the conversion of the remaining S_4N_4 to S_2N_2. The product, formed in the vapour phase, is slowly sublimed at room temperature, which generates high quality crystals of pure diamagnetic S_2N_2. The resulting crystals are initially colourless, but soon become blue-black, and, ultimately golden in colour as S_2N_2 spontaneously polymerizes and forms the superconducting sulphur nitride polymer, $(SN)_x$.[92]
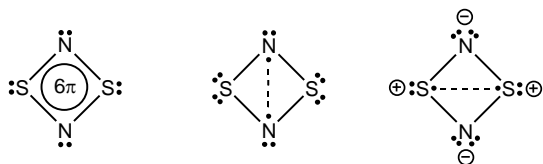
24

Although S_2N_2 is perhaps best know for its role in the production of $(SN)_x$,[93] its rather peculiar bonding arrangement renders it an interesting species in its own right. S_2N_2 has a square planar ring structure in with alternating sulphur and nitrogen atoms.[94] Over the past 30 years, several theoretical studies have attempted to elucidate the uncertainties associated with its electronic structure:[95] Is the molecule aromatic like the valence isoelectronic cyclobutadiendiide anion, or is it perhaps closer to the diradical structure of cyclobutane-1,3-diyl **16**? In addition, the N and S units in **24** are formally isoelectronic with CH and CH_2, respectively, as are S^+ and N^-. Consequently, *two* different diradical structures that are analogous to cyclobutane-1,3-diyl can be drawn for S_2N_2 (see above).

The planar molecular structure, the number of π-electrons, and results from different level MO theory calculations all speak in favour of the aromaticity of S_2N_2.[95a,b,j] However, classical valence bond (VB) calculations have indicated that the primary Lewis-type structure for S_2N_2 is a spin-paired singlet diradical with a long transannular N···N interaction.[95c–e,i] Conversely, spin-coupled VB theory calculations have shown that while the structure is a singlet diradical in nature, the diradical

character should be assigned to the sulphur rather than the nitrogen atoms.[95g] Consensus regarding the electronic structure of S_2N_2 has yet to be reached.

3.3.7 Tetrachalcogen dications Ch_4^{2+} (Ch = S, Se, Te)

The diamagnetic group 16 polycations Ch_4^{2+} (Ch = S, Se, Te) (**25**) have all been known experimentally for a number of years.[96] They can be prepared by, for example, oxidizing the corresponding elements with excess SbF_5. X-ray crystal structure determinations have confirmed that the cations have similar square planar structures with four Ch–Ch bonds of equal length and bond angles close to 90°.
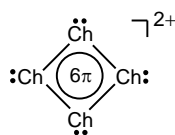
25

Although the electronic structures of **25** appear to be closely related to the other four-membered ring systems described above, their possible diradical nature has been overlooked in the past. In the majority of cases, the dications have been assumed to be aromatic based on MO calculations at the RHF level of theory, or simply because they fulfill the Hückel criteria of aromaticity. In consequence, delocalized π-structures have been used to describe their bonding.[97] This oversimplification is surprising considering that on many occasions they have been described as computationally difficult systems displaying strong electron correlations.[98] Only a few VB theory studies that address the diradical character of **25** have been undertaken.[95d,99]

3.4 Quantification of singlet diradical character

A question of great significance which as yet remains unanswered is, whether it is possible to easily quantify the diradical character of systems discussed above. Although the exceptional stabilities reported already hint at vastly reduced radical characters, a more quantitative index is required in order to evaluate their value with respect to practical applications. After all, the main research endeavour is to synthesize diradicaloids which are not only stable, but which display as much diradical character as possible.

3.4.1   Available methodologies

Due to the nature of the problem, the majority of methods applicable to quantify singlet diradical character are theory-based: diradical character is not a physical observable, but a property of the wave function which provides informative insight into the chemical characteristics of the investigated systems. Perhaps the only means which (in principle) can also be applied in practice is to use the energy difference between the lowest singlet and triplet states as an indicator of the diradical character. A small singlet-triplet splitting generally corresponds to a minute coupling between the two electrons and, therefore, to a large singlet diradical character. The inverse is naturally true as well. However, the singlet-triplet energy splitting is by no means the only factor governing the diradical nature of a given system. Also, although the maximum point for such a scale is easily defined − with zero singlet-triplet splitting corresponding to 100% diradical character − no clear-cut definition for 0% diradical character can be made.

Other attempts to determine the extent of singlet diradical character have been based on orbital overlap,[100] the magnitude of spin contamination for symmetry-broken unrestricted singlet SCF solutions,[101] and the energy difference between restricted and symmetry-broken unrestricted singlet SCF solutions.[102,xxii,103] Although all the aforementioned methods are capable of identifying singlet diradical character in molecular systems, they, like the singlet-triplet separation-based method, suffer from problems related to constructing a legitimate scale.

Two of the most theoretically robust methods for determining the amount of singlet diradical character are based on the analysis of the multiconfigurational wave function.[104] The CI treatment for the dissociation of the H_2 molecule using minimal basis provides an illustrative example.[24]

Close to the equilibrium bond distance r_e, H_2 is well-described with a RHF-type wave function

$$\Phi_{RHF} = \phi_B(1)\phi_B(2), \tag{3.11}$$

in which $\phi_B = \chi_1 + \chi_2$ is the bonding MO, and χ_i is the s-type AO on nuclei i; the spin function and normalization coefficients have been ignored. Consequently, in a CI wave

---

xxii A new orbital-based definition for multiradical character of molecular systems was recently formulated.[103]

function, the CI coefficient for the RHF configuration is close to unity, and that of the doubly excited (DE) configuration Φ_{DE} is essentially zero. Hence,

$$\begin{aligned}\Phi_{CI} &= c_{RHF}\Phi_{RHF} + c_{DE}\Phi_{DE} \\ &= c_{RHF}[\phi_B(1)\phi_B(2)] + c_{DE}[\phi_{AB}(1)\phi_{AB}(2)] \approx \Phi_{RHF}.\end{aligned} \tag{3.12}$$

When the H–H bond is lengthened, the RHF wave function becomes a gradually poorer approximation of the system since it includes an equal amount of ionic and covalent contributions, and cannot properly describe the increasing singlet diradical character. An improved description of the system is given by the CI method which allows the doubly excited, antibonding, configuration

$$\Phi_{DE} = \phi_{AB}(1)\phi_{AB}(2) \tag{3.13}$$

to enter the wave function. At each bond distance considered, the optimum values for the coefficients c_{RHF} and c_{DE} in Equation (3.12) are determined by the variational procedure. The more the bond is stretched, the bigger the coefficient c_{DE} will become and the further the CI wave function is from the RHF reference function.

At infinite H–H separation, the system becomes a pure diradical and the ionic contributions in the wave function must vanish. This can happen only if $c_{RHF} = -c_{DE} = 2^{-\frac{1}{2}}$ as evident from the CI function written in terms of atomic orbitals

$$\begin{aligned}\Phi_{FCI} &= c_{RHF}[\phi_B(1)\phi_B(2)] + c_{DE}[\phi_{AB}(1)\phi_{AB}(2)] \\ &= c_{RHF}[(\chi_1(1) + \chi_2(1))((\chi_1(2) + \chi_2(2)))] \\ &\quad + c_{DE}[(\chi_1(1) - \chi_2(1))((\chi_1(2) - \chi_2(2)))] \\ &= (c_{RHF} + c_{DE})[\chi_1(1)\chi_1(2) + \chi_2(1)\chi_2(2)] \\ &\quad + (c_{RHF} - c_{DE})[\chi_1(1)\chi_2(2) + \chi_2(1)\chi_1(2)].\end{aligned} \tag{3.14}$$

A useful index for the diradical character of a molecule can then be defined as the ratio

$$\frac{(c_{DE})^2}{(2^{-\frac{1}{2}})^2}(\times 100\%) = 2(c_{DE})^2\left(\times 100\%\right) \tag{3.15}$$

which approaches unity (100%) for pure diradicals and zero (0%) for typical closed-shell singlet states.[104a] The aforesaid is illustrated graphically in Figure 3.5.
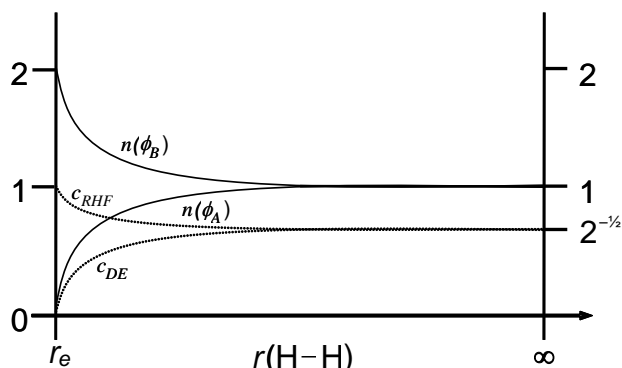
Figure 3.5 Variation of CI coefficients and natural orbital occupation numbers with respect to H−H bond length in H_2; minimum basis set description.

An alternative index for quantifying diradical character is provided by the natural orbital occupation numbers[xxiii] of the two orbitals associated with the radical nature.[104b] The more closely the orbital occupation numbers approach each other, the closer the system is to a pure diradical. For the quantum mechanical guinea-pig H_2, the CI natural orbital occupation numbers n of bonding $n(\phi_B)$ and antibonding $n(\phi_{AB})$ orbitals at equilibrium bond distance are 1.98 and 0.02, respectively. At infinite separation of the nuclei, each of the occupation numbers approaches unity, thus indicating that the system is essentially a pure diradical (see Figure 3.5).

To employ either one of the above measures of diradical character requires that multiconfigurational wave functions be used. Naturally, the results are dependent upon the quality of the wave function *i.e.* the chosen MCSCF approach. If small active spaces such as the two-configuration space are used, both of these methods tend to greatly overestimate diradical character. Thus, active spaces comparable to the size of the full valence space should be used to obtain close to converged results. Also, diradical character determined from natural orbital occupations is always larger than what can be inferred from the CI coefficients. This is due to the fact that the orbitals associated with the diradical nature also appear in configuration state functions other than the two related to the diradical character. The quantification method based on CI coefficients was used in Papers **V** and **VI**.

[xxiii] Natural orbitals are those which diagonalize the one-particle density matrix, and the natural orbital occupation numbers are its eigenvalues.

3.4.2 Computational results

Quantum chemical calculations describing the organic parent diradical **16** in its lowest singlet state have demonstrated that its natural orbital occupations are approximately 1.20 and 0.90.[90a] This corresponds to a diradical character of 85%. In other words, a planar singlet cyclobutane-1,3-diyl − if it existed − would be an almost pure diradical.

Studies describing the singlet diradical character of inorganic systems discussed in the previous sections (other than **21**) are scarce. A CAS(2,2) calculation for the model system of **15**, $(HP)_2(CH)_2$, has indicated the presence of a significant amount of diradical character; the CI coefficient for the doubly excited configuration is 0.40 which corresponds to a natural orbital occupations of 1.70 and 0.30, and to a diradical character of more than 30%.[1a] Such a large value is most likely an overestimation of the true amount because it is based on calculations using the smallest possible active space size. No data has been reported for other derivatives of **15** or for other 2,4-diphospha-cyclobutane-1,3-diyls **18**−**20**.

For diradicaloids with heavier group 14 atoms, the only reported data are the singlet-triplet energy splittings.[1c,d] A comparison of these values to the singlet-triplet splitting calculated for the model system of **15**, approximately 25 kJ mol^{-1},[1a] indicates that radical electrons in **22** and **23** are expected to be considerably more strongly coupled than in **15**.

The largest amount of data regarding the quantification of diradical character has been published for 1,3-dibora-2,4-diphosphonio-cyclobutane-1,3-diyls **21**.[90] This is perhaps due to the somewhat provocative way in which such systems were initially described; the synthesized derivative was reported to be a singlet diradical which is "indefinitely stable at room temperature both in solution and in the solid state".[1b] Quantum chemical calculations later demonstrated that compounds **21** possess no more than moderate diradical character and are stable only due to their dominant bonding character.[90] For example, the published natural orbital occupation numbers of the parent system $(H_2P)_2(BH)_2$ are 1.77 and 0.23, which indicates that it has approximately 20% diradical character. This value is less that what has been determined for **15**, but still much more than what is typical for normal closed-shell molecules (a few percent).

Although the extant theoretical data regarding the diradical nature of compounds **15**−**25** is far from complete, the number of examples described above already illustrates

the substantial variation in diradical character when going from one system to another. It seems logical to ask why these compounds have significantly different amounts of diradical character even though they share qualitatively similar valence isoelectronic structures. The answer obviously lies in the orbital energy difference between the HOMO and LUMO (*vide supra*). Several theoretical studies analysing the factors which govern the orbital energy separation in these diradicals have recently been published.[90a,b;105] The results demonstrate that general trends can be inferred using standard orbital mixing arguments; the four-membered ring moieties can be sub-divided into smaller fragments whose mutual π-orbital interactions largely determine the resulting HOMO–LUMO gap and, thus, also the amount of diradical character. In addition to the orbital interactions within the π-system, the other key factor which affects the diradical nature of these systems is the electron-withdrawing *vs.* electron-donating role of the substituents attached to the ring atoms.

These matters were also discussed in Papers **V** and **VI** in which the electronic structures and diradical characters of S_2N_2, chalcogen dications Ch_4^{2+} (Ch = S, Se, Te), and some other related systems were analysed using multiconfigurational methods.

3.5   Results and discussion

The following sections review the most important results published for the most part in Papers **V** and **VI**.

3.5.1   The electronic structure of S_2N_2

The electronic structure of S_2N_2 has been a source of great controversy in the past. The employment of different theoretical methods has led to diverse interpretations, and opinions regarding the best description of its electronic structure have gone back and forth between an aromatic system and a singlet diradical.[95] It is rather interesting to note that not a single multiconfigurational MO wave function-based analysis of its electronic structure has been published; the studies which indicate S_2N_2 to be a singlet diradical have all been based on VB theory calculations.[95d,e,g–i] If S_2N_2 truly has significant diradical character, proper theoretical treatment is paramount in calculations of its molecular properties. Typical MO methods such as RHF and second-order Møller-

Plesset perturbation theory (MP2) are incapable of treating static electron correlation and produce meaningless results in cases where these effects are significant.[24]

In Paper **V** the electronic structure of S_2N_2 was analysed using various theoretical approaches. The RHF wave function for S_2N_2 shows the existence of four σ-bonding MOs and three occupied π-orbitals of which only one is bonding throughout the ring. The two other π-orbitals are nonbonding and are the highest occupied MOs with nearly equal energies. Thus, S_2N_2 appears to be an aromatic system with six π-electrons and a formal bond order of 1.25. Such a result compares favourably with the delocalized view of bonding in S_2N_2. However, SCF stability analysis indicates that the RHF wave function is unstable with respect to orbital double occupation and a lower-energy, symmetry-broken, singlet UHF solution to the SCF equations exists. Consequently, S_2N_2 appears to have some diradical character in its wave function.

An inspection of the symmetry-broken UHF wave function (presented in detail in Paper **V**) gives a good zero-order approximation of the origin of the diradical character: the UHF wave function has lower symmetry than the molecular framework and, consequently, two orbitals which show two singlet-coupled electrons each of which is localized on one of the nitrogen centres. The localization of electrons on the radical sites is also visible in the UHF spin density which naturally mirrors the composition of the orbitals. In order to quantify the radical character in S_2N_2, CAS calculations were carried out using the full valence space − 22 electrons in 16 orbitals − as active (see Paper **V**). The calculated CI coefficients for the RHF and the doubly excited configurations are 0.93 and −0.18, respectively, which correspond to 6% diradical character. The relevant natural orbital occupation numbers are 1.90 and 0.14, and they compare well with the CI coefficients. In consequence, the analysis of the CAS wave function indicates that the diradical character of S_2N_2 reduces its delocalized, aromatic, nature by less than 10%. For comparison, the most recent VB studies have shown that the N···N diradical structure has 47% weight in the VB wave function of S_2N_2.[95i] At first glance, such a large value seems to be a clear contradiction of the results obtained from the CAS MO wave function. This mode of thinking, however, represents a general misconception which is encountered far too often.

Although at a sufficiently high level of theory both VB- and MO-based approximations converge to an equal solution *i.e.* they give the same total energies and

electron densities, the descriptions of bonding yielded by these two methods remain vastly different.[24] For example, in MO theory the π-system of benzene is described with six highly delocalized MOs whereas the corresponding VB orbitals are highly localized, almost pure p-orbitals on carbon atoms. From the MO standpoint, the increased stability of benzene can be attributed to the large energy gap between the HOMO and LUMO orbitals. In VB theory, the stability of benzene is attributed to resonance between five different VB structures. However, the VB resonance energy cannot be obtained from the MO wave function; nor can the HOMO–LUMO stabilization energy be determined from a VB calculation. Thus, it is important that the concepts used to describe molecular bonding in one approach are not directly compared to those utilized in another method.

Returning to the elucidation of the diradical character of S_2N_2, a simple means to verify that the CAS and VB results truly coincide does exist: because both wave functions are multiconfigurational, either one of them can be easily expressed in terms of the other (see Paper **V**). Results from a qualitative, back-of-the-envelope-type calculation for S_2N_2 show that the N$\cdots$N diradical VB structure has a 34% weight in the CAS wave function, whereas the weight for the S$\cdots$S diradical structure is only 14%. The reported VB weights for the two Lewis structures are 47% and 6%.[95i] Indeed, the qualitative agreement between these results is excellent, which strengthens the interpretation that S_2N_2 is primarily an aromatic system with a small amount of diradical character that can be assigned solely to the nitrogen atoms.[xxiv]

Shortly after the submission of Paper **V** for publication, the first multiconfigurational studies analysing the electronic structure of S_2N_2 were reported.[95j] The published results are, not surprisingly, essentially identical to ones reported here and in Paper **V**: S_2N_2 is mainly an aromatic π-system since it satisfies the energetic, structural and magnetic criteria for aromaticity, but it also displays some "strong antibonding electron correlations" which reduce its aromatic character by approximately 7%. Quite surprisingly the authors did not relate these antibonding electron correlations with the diradical character of S_2N_2 – in fact, it was concluded that the diradical character in S_2N_2 is insignificant.

[xxiv] It should be obvious at this point that the VB structural weights cannot be used to quantify diradical character in a similar fashion as CI coefficients from a CAS calculation.

The primary evidence by which it was inferred that the diradical character in S_2N_2 is negligible was the lack of a symmetry-broken unrestricted Kohn-Sham solution.[95j] However, as discussed earlier, this is not a sufficient proof: any conclusions regarding the singlet diradical nature of molecules must be made based on the analysis of the true wave function, not the reference determinant used in DFT calculations. This obvious misinterpretation of theory was discussed more thoroughly in Paper **VI**.

Answers to the question concerning the general significance of the diradical character in S_2N_2 were also sought in Papers **V** and **VI**. While it is certainly tempting to deem the amount insignificant,[95j] calculations of second- and higher-order molecular properties of S_2N_2 demonstrated that the inclusion of even such a small amount of diradical character to the wave function is essential in order to obtain reliable results. If the diradical character is omitted by using a RHF zero-order wave function, the use of a perturbational approach to calculate dynamic electron correlation effects is no longer justifiable, and spurious results are obtained at the MP2 level.[24] Also, the higher the order of the calculated property, the more profound the errors become: single configuration-based methods give reasonable geometries and even qualitatively correct vibrational frequencies, but are doomed to fail in predicting properties such as IR intensities, Raman activities, and NMR chemical shifts. A more detailed example is given below in the context of chalcogen dications.

3.5.2   Heavy-atom analogues of S_2N_2

A considerable amount of research has been directed toward the synthesis of heavier-chalcogen analogues of polymeric sulphur nitride, as they are expected to display increased conductivities relative to $(SN)_x$. At present, only two potential methods leading to the selenium and mixed selenium-sulphur polymers $(SeN)_x$ and $(SeNSN)_x$ are being investigated.[106] Since both proposed routes involve Se_2N_2 or $SeSN_2$ ring systems as reaction intermediates, molecular characterization methods capable of identifying the four-membered rings will be crucial in determining whether the synthetic approaches are viable or not. High-level theoretical calculations can play an important role in providing accurate data regarding the molecular properties of Se_2N_2 and $SeSN_2$ to which the experimental results can then be compared.

The electronic structures and molecular properties of Se_2N_2 and $SeSN_2$ were analysed in Paper **VI**. The CI vector coefficients from CAS(22,16) calculations revealed that the selenium systems possess only a few per cent more diradical character than S_2N_2. Consequently, their diradical nature should not pose any more difficulties for their isolation as stable molecular entities than what already exists due the inherent thermal lability of Se=N double bonds.[107] Paper **VI** also reports high-level computational results for the structures, vibrational frequencies, IR intensities, Raman activities, NMR chemical shifts, and excitation energies of Se_2N_2 and $SeSN_2$. The spectroscopic data, which will not be discussed anew here, are of considerable value in efforts aimed at the preparation of the conducting polymers $(SeN)_x$ and $(SeNSN)_x$.

3.5.3   Chalcogen dications Ch_4^{2+} (Ch = S, Se, Te)

In Paper **V**, the electronic structures of the tetrachalcogen dications Ch_4^{2+} (Ch = S, Se, Te) were compared with results obtained for disulphur dinitride. It was shown that the RHF wave function is an even worse approximation for the electronic ground state of these dications than it is for that of S_2N_2: the RHF configuration has only 80% weight in the CAS CI expansion of Ch_4^{2+} cations. In addition, the highest occupied orbitals in Ch_4^{2+} are energetically degenerate as a consequence of fourfold symmetry, and the CAS wave function includes two equally important diradical configurations which correspond to the two different Lewis-type VB diradical structures that can be drawn for Ch_4^{2+}. The diradical character was found to increase slightly in the order $S_4^{2+} < Se_4^{2+} < Te_4^{2+}$.

The prediction of ^{77}Se NMR chemical shift of Se_4^{2+} with theoretical methods offers an illustrative example of the importance of proper treatment of static electron correlation effects in these systems. The reported RHF and MP2 chemical shifts of Se_4^{2+} are 3821 and 154 ppm, respectively.[98b] Comparison with the experimental value of 1936 ppm shows that both methods completely fail to describe the system, since deviations from experiment are roughly ± 2000 ppm. In contrast to the unsatisfactory performance of both RHF and MP2, a recent DFT study reported a calculated chemical shift of 1834 ppm for Se_4^{2+}.[98a] Apparently the chosen density functional is capable of describing the moderate static electron correlation effects involved, and the calculated value compares favourably with the experimentally observed chemical shift.

The poor performance of RHF and MP2 is not surprising if the singlet diradical character of Se_4^{2+} is taken into account. It is obvious that multiconfigurational methods are needed if improved results are sought with wave function-based methods. The results reported in Papers **V** and **VI** show that CAS calculations using the full active space give a remarkably good agreement with the experimental value: a chemical shift of 1893 ppm was calculated for Se_4^{2+}. Pure density functionals yielded equally accurate values as CAS, but hybrid functionals gave results that were overestimated by several hundred ppm.

The calculated ^{77}Se NMR chemical shifts for the mixed sulphur-selenium cations with the composition $S_xSe_{4-x}^{2+}$ (x = 1–3) were also reported in Paper **V** (see Figure 3.6). Both CAS and DFT results (using pure functionals) were in excellent agreement with the experimental values[108] which thereby confirms the experimental assignment of resonances and ensures that the good performance of these methods in predicting the chemical shift of Se_4^{2+} is more than fortuitous.
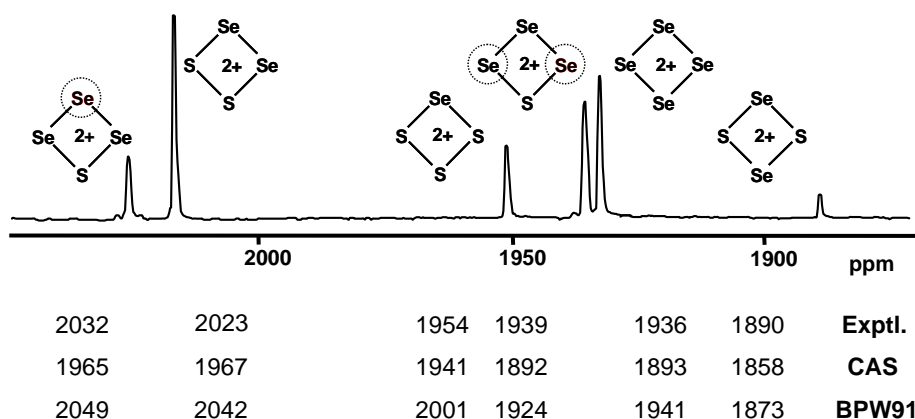

2032	2023	1954	1939	1936	1890	**Exptl.**
1965	1967	1941	1892	1893	1858	**CAS**
2049	2042	2001	1924	1941	1873	**BPW91**

Figure 3.6 Calculated and experimental ^{77}Se chemical shifts of $S_xSe_{4-x}^{2+}$ (x = 0–3).

Hybrid functionals include a constant fraction of the exact RHF exchange which is a reasonable approximation for most regular systems, but not for singlet diradicals.[25] For example, in the case of a dissociated H_2 molecule, the exchange-correlation hole is localized and removes exactly one electron from the proton where the reference electron is located, while being zero at the other nucleus. In such a situation, mixing any amount of delocalized exact exchange to the description is simply incorrect and will lead to

unphysical delocalized exchange-correlation holes; the same also applies for the singlet diradicaloids discussed herein. Thus, pure density functionals which use local descriptions of the exchange-correlation hole yield better results for singlet diradicaloids than hybrid functionals.

The previous example demonstrates how deceptive density functional methods can sometimes be. If experimental data were not available for comparison, nothing else in the calculations with hybrid functionals would give an indication of possible errors in the results, as even the stability analysis yields all positive eigenvalues. Thus, caution should always be exercised when DFT is used to study systems in which diradical character is expected to differ significantly from zero.

3.5.4   Other inorganic main group singlet diradicaloids

As discussed earlier, the data used to quantify the singlet diradical nature of main group systems based on cyclobutane-1,3-diyl are incoherent. Various approaches have been used for different systems which impedes the direct comparison of results. For example, CAS CI coefficients have been reported only for the parent system of **15**,[1a] whereas no more than calculated singlet-triplet energy differences are available for **22** and **23**.[1c,d] Most of the results are also based on two-configuration wave functions which greatly overestimate diradical character.

To get a better overview of the situation, diradical characters of systems **15**, **21**, **22**, and **23** were calculated using CI coefficients from CAS(22,16) optimizations. Only model compounds in which organic groups and halogens are replaced with hydrogen atoms were used in the calculations. The active space used is slightly smaller than the full valence space for these systems, but represents the largest possible choice feasible for such calculations. Thus, absolute values are expected to be a few per cent in error. More importantly, these results allow − for the first time − an accurate comparison of the relative diradical character between the different systems.

The largest diradical character is, quite surprisingly, observed for species **22**, at 21%; the analogous tin system has a diradical character of 11%. Both **15** and **21** have similar amounts of diradical character, at 13% and 15%, respectively. Although the calculations were done for model systems, it is reasonable to expect that the relative

ordering of the diradical character of these systems will remain the same if the substituents are changed to simple organic groups such as Me, ^{i}Pr, or ^{t}Bu.

The diradical characters reported herein show that the previously reported CAS(2,2) results for **15** have led to somewhat unfounded claims regarding its diradical character.[1a] The calculated value is still more what would be expected for a simple closed-shell system, but it is much less than what is calculated for *e.g.* **22**. In fact, compounds of the type **15** seem to be intrinsically no better singlet diradicaloids than the highly disputed species **21**. Although the above result contradicts the claims made earlier, the diradical characters calculated from the CAS(22,16) wave functions are in good agreement with the stabilities reported for these systems.[1] Also, systems **15** and **21** have been found to be non-reactive towards solvents whereas compound **22** reacts readily with benzene, toluene, and cyclohexane.[1]

The experimentally known inorganic analogues of cyclobutane-1,3-diyl are by no means the only possible main group diradicaloid systems that can be envisaged. Perhaps one of the most interesting candidates is the cyclic P_2O_2 system. Calculations at multiconfigurational levels have shown that its diradical character should be comparable to that of **22** and **23**.[109] However, the absence of steric protection at the radical centres suggests that its isolation as a stable entity might prove difficult, or even impossible. Theoretical analyses have also predicted that the replacement of the "PR_2^+" fragments in **21** by isoelectronic "NR_2^+" units should double its diradical character.[105] A drastic increase in the diradical character of **21** is also anticipated if more electron-donating substituents, such as silyl rather than alkyl groups, are introduced at the phosphorus centres.[105] Thus, it seems reasonable to say that the inorganic main group analogs of cyclobutane-1,3-diyl with maximized diradical character still await discovery.

Chapter 4

Conclusions

Main group radicals have many potential applications as a result of their net magnetic moment which arises from the spin of the unpaired electron(s). They are, however, often difficult to characterize experimentally because of their prevalent persistent nature and complex EPR spectra originating from the hyperfine coupling of the unpaired electron(s) to a number of magnetically active nuclei with multiple isotopes. Viable remedies to the former are efficient delocalization of the unpaired electron(s) and the use of sterically encumbered substituents to prevent molecular coupling reactions. The latter problem can be greatly simplified by using quantum chemical calculations to aid in the spectral analyses.

The results reported in this thesis clearly demonstrate the capability of density functional methods to predict hyperfine coupling constants that are in almost quantitative accuracy with the experimental values. The calculated coupling constants can subsequently be incorporated into a simulation of the experimental EPR spectrum, which, once optimized, yields an accurate description of the magnetic hyperfine interactions and, consequently, of the spin distribution in a paramagnetic molecule. Through this combination of experimental and theoretical methods, the current research project provided fundamental information about stable and persistent main group radicals involving some novel polyimido anions of phosphorous, as well as metal complexes of the boraamidinate ligand. This bedrock of data is essential for future

studies of the incorporation of these radicals into useful materials. The studies on paramagnetic gallium complexes of the 1,4-diaza-1,3-butadiene ligand not only enabled the accurate interpretation of their EPR spectra, but provided important insight into their electronic structures and the interpretation of spectroscopic data reported for some related paramagnetic group 13 metal complexes.

The theoretical first-principles treatment of singlet diradicals and diradicaloids is a challenging quantum chemical task. The computational results discussed in this thesis present a particularly illustrative example of how quantum chemical treatment of molecules having only a minute amount of singlet diradical character requires the proper use of advanced methodologies; only methods which are capable of treating the important configurations in their wave function adequately and equally ensure that reliable results are obtained. This prerequisite has been highly overlooked in the past which has lead to unnecessary confusion regarding the electronic structure of S_2N_2, problems in predicting the ^{77}Se NMR chemical shift of Se_4^{2+}, and to disputable claims about the diradical characters of 2,4-diphosphacyclobutane-1,3-diyls and 1,3-dibora-2,4-diphosphoniocyclobutane-1,3-diyls.

The analysis of the electronic structures of inorganic singlet diradicaloids mimicking cyclobutane-1,3-diyl showed that they range from almost aromatic to only moderately diradicaloid. Despite the predominantly closed-shell nature of the synthesized species, various experimental and theoretical studies hitherto undertaken provide a solid groundwork for future research projects directed towards maximising their singlet diradical character. This is not an insuperable task, as the periodic table offers many more combinations of the atoms in the inorganic analogues of cyclobutane-1,3-diyl. Thus, major developments in the field of stable main group singlet diradicaloids are highly anticipated in the foreseeable future.

Bibliography

1   (a) Niecke, E.; Fuchs, A.; Baumeister, F.; Nieger, M.; Schoeller, W. W. *Angew. Chem., Int. Ed. Engl.* **1995**, *34*, 555. (b) Scheschkewitz, D.; Amii, H.; Gornitzka, H.; Schoeller, W. W.; Bourissou, D.; Bertrand, G. *Science* **2002**, *295*, 1880. (c) Cui, C.; Brynda, M.; Olmstead, M. M.; Power, P. P. *J. Am. Chem. Soc.* **2004**, *126*, 6510. (d) Cox, H.; Hitchcock, P. B.; Lappert, M. F.; Pierssens, L. J.-M. *Angew. Chem., Int. Ed.* **2004**, *43*, 4500.

2   See, for example: *Spin Labelling: Theory and Applications Vol. 2*, (Ed.: Berliner, L. J.), Academic Press, 1979.

3   See, for example: Hawker, C. *Acc. Chem. Res.* **1997**, *30*, 373.

4   See, for example: (a) Sheldon, R. A. *Acc. Chem. Res.* **2002**, *35*, 774. (b) Bar-On, B.; Mohsen, M.; Zhang, R.; Feigin, E.; Chevion, M.; Samuni, A. *J. Am. Chem. Soc.* **1999**, *121*, 8070.

5   See, for example: (a) Stubbe, J.; van der Donk, W. A. *Chem. Rev.* **1998**, *98*, 705. (b) Stubbe, J. *Chem. Commun.* **2003**, 2511. (c) Bastian, N. R.; Foster, M. J. P.; Ballantyne, M.; Lu, Y. *Curr. Top. Biophys.* **2002**, *26*, 115.

6   See, for example: (a) *Magnetic Properties of Organic Materials*, (Ed.: Lahti, P. M.), Marcel Dekker, 1999. (b) Low, P. J. *Dalton Trans.* **2005**, 2821. (c) Lemaire, M. T. *Pure Appl. Chem.* **2004**, *76*, 277.

7   Gomberg, M. *J. Am. Chem. Soc.* **1900**, *22*, 757.

8   For recent reviews, see: (a) Tidwell, T. T. *Adv. Phys. Org. Chem.* **2001**, *36*, 1. (b) Power, P. P. *Chem. Rev.* **2003**, *103*, 789.

9   For some of the most recent reports, see: (a) Tumanskii, B.; Pine, P.; Apeloig, Y.; Hill, N. J.; West, R. *J. Am. Chem. Soc.* **2005**, *127*, 8248. (b) Nakamoto, M.; Yamasaki, T.; Sekiguchi, A. *J. Am. Chem. Soc.* **2005**, *127*, 6954. (c) Makarov, A. Y.; Irtegova, I. G.; Vasilieva, N. V.; Bagryanskaya, I. Y.; Borrmann, T.; Gatilov, Y. V.; Lork, E.; Mews, R.; Stohrer, W.-D.; Zibarev, A. V. *Inorg. Chem.* **2005**, *44*, 7194. (d) Beer, L.; Brusso, J. L.; Haddon, R. C.; Itkis, M. E.; Leitch, A. A.; Oakley, R. T.; Reed, R. W.; Richardson, J. F. *Chem. Commun*, **2005**, 1543.

10   For a review, see: Lappert, M. F.; Lednor, P. W. *Adv. Organomet. Chem.* **1976**, *14*, 345.

11   A textbook which gives a good overview of the recent developments in the field of magnetic resonance and presents the available theoretical methods in detail is: *Calculation of NMR and EPR Parameters: Theory and Applications* (Eds.: Kaupp, M.; Bühl, M.; Malkin, V. G.), Wiley VCH, 2004.

12   See Chapters 29, 30, and 35 in Reference 11.

13   See Chapters 30 and 35 in Reference 11.

14   See Chapters 5 and 29 in Reference 11.

15   The theoretical treatment in Section 2.1 is adopted from: Weil, J.; Bolton, J. R.; Wertz, J. E. *Electronic Paramagnetic Resonance: Elementary Theory and Practical Applications*, Wiley, 1994.

16   See Chapter 31 in Reference 11.

17   Meyer, W. *J. Chem. Phys.* **1969**, *51*, 5149.

18   For recent benchmarks, see: (a) Barone, V. in *Recent Advances in Density Functional Methods*, *Vol. 1*, (Ed.: Chong, D. P.), World Scientific, 1996. (b) Hermosilla, L.; Calle, P.; Garcia de la Vega, J. M.; Sieiro, C. *J. Phys. Chem. A* **2005**, *109*, 1114.

19   For a recent benchmark, see: Nguyen, M. T.; Creve, S.; Vanquickenborne, L. G. *J. Phys. Chem. A* **1997**, *101*, 3174.

20   See, for example, the analysis reported in: Helgaker, T.; Jaszuński, M.; Ruud, K.; Górska, A. *Theor. Chem. Acc.* **1998**, *99*, 175.

21   See Chapter 35 in Reference 11.

22   See Chapter 29 in Reference 11.

23   See, for example: Kobus, J.; Quiney, H. M.; Wilson, S. *J. Phys. B: At. Mol. Opt. Phys.* **2001**, *34*, 2045.

24   The discussions regarding wave function methods in Sections 2.2, 3.2, and 3.4 are adopted from: (a) Jensen, F. *Introduction to Computational Chemistry*, Wiley, 1999. (b) Helgaker, T.; Jørgensen, P.; Olsen, J. *Molecular Electronic Structure Theory*, Wiley, 2000.

25   The discussions regarding density functional methods in Sections 2.2 and 3.2 are adopted from: Koch, W.; Holthausen, M. C. *A Chemist's Guide to Density Functional Theory*, *2nd Edition*, Wiley VCH, 2001.

26   See Chapter 30 in Reference 11.

27   See, for example, the analysis presented in: Laming, G. J.; Handy, N. C.; Amos, R. D. *Mol. Phys.* **1993**, *80*, 1121.

28   See, for example: Munzarová, M.; Kaupp, M. *J. Phys. Chem. A* **1999**, *103*, 9966.

29   (a) Fernandez, B.; Jørgensen, P.; Byberg, J.; Olsen, J.; Helgaker, T.; Jensen, H. *J. Chem. Phys.* **1992**, *97*, 3412. (b) Rinkevicius, Z.; Telyatnyk, L.; Vahtras, O.; Ågren, H. *J. Chem. Phys.* **2004**, *121*, 7614.

30   For a recent benchmark, see: Arbuznikov, A. V.; Kaupp, M.; Malkin, V. G.; Reviakine, R.; Malkina, O. L. *Phys. Chem. Chem. Phys.* **2002**, *4*, 5467.

31   For recent reviews, see: (a) Brask, J. K.; Chivers, T. *Angew. Chem., Int. Ed.* **2001**, *40*, 3960. (b) Aspinall, G. M.; Copsey, M. C.; Leedham, A. P.; Russell, C. A. *Coord. Chem. Rev.* **2002**, *227*, 217.

32   For a review, see: Chivers, T. *Top. Curr. Chem.* **2003**, *229*, 143.

33   Niecke, E.; Frost, M.; Nieger, M.; von der Gönna, V.; Ruban, A.; Schoeller, W. W. *Angew. Chem., Int. Ed. Engl.* **1994**, *33*, 2111.

34   Steiner, A.; Zacchini, S.; Richards, P. I. *Coord. Chem. Rev.* **2002**, *227*, 193.

35   (a) Raithby, P. R.; Russell, C. A.; Steiner, A.; Wright, D. S. *Angew. Chem., Int. Ed. Engl.* **1997**, *36*, 649. (b) Armstrong, A.; Chivers, T.; Krahn, M.; Parvez, M.; Schatte, G. *Chem. Commun.* **2002**, 2332.

36   (a) Fleischer, R.; Freitag, S.; Pauer, F.; Stalke, D. *Angew. Chem., Int. Ed. Engl.* **1996**, *35*, 204. (b) Fleischer, R.; Freitag, S.; Stalke, D. *J. Chem. Soc., Dalton Trans.* **1998**, 193. (c) Chivers, T.; Parvez, M.; Schatte, G. *Inorg. Chem.* **1996**, *35*, 4094. (d) Brask, J. K.; Chivers, T.; McGarvey, B.; Schatte, G.; Sung R.; Boeré, R. T. *Inorg. Chem.* **1998**, *37*, 4633.

37   Armstrong, A.; Chivers, T.; Parvez, M.; Boeré, R. T. *Angew. Chem., Int. Ed.* **2004**, *42*, 502.

38   Armstrong, A.; Chivers, T.; Parvez, M.; Schatte, G.; Boeré, R. T. *Inorg. Chem.* **2004**, *43*, 3459.

39   (a) Hughes, K. W. E.; Moulton, W. G. *J. Chem. Phys.* **1963**, *39*, 1359. (b) Maruthamuthu, P.; Neta, P. *J. Phys. Chem.* **1978**, *82*, 710.

40   For a recent review of phosphorus-containing radicals, see: Armstrong, A.; Chivers, T.; Boeré, R. T. in *Modern Aspects of Main Group Chemistry*, (Eds.: Lattman, M.; Kemp, R. A.), ACS Symposium Series 917, 2005.

41 For reviews, see: (a) Edelmann, F. T. *Coord. Chem. Rev.* **1994**, *137*, 403. (b) Barker, J.; Kilner, M. *Coord. Chem. Rev.* **1994**, *133*, 219.

42 Duchateau, R.; Meetsma, A.; Teuben, J. H. *Chem. Commun.* **1996**, 223.

43 Dagome, S.; Guzei, I. A.; Coles, M. P.; Jordan, R. F. *J. Am. Chem. Soc.* **2000**, *122*, 274.

44 (a) Brussee, E. A. C.; Meetsma, A.; Hessen, B.; Teuben, J. H. *Chem. Commun.* **2000**, 497. (b) Brussee, E. A. C.; Meetsma, A.; Hessen, B.; Teuben, J. H. *Organometallics* **1998**, *17*, 4090.

45 For a recent review, see: Blais, P.; Brask, J. K.; Chivers, T.; Fedorchuk, C.; Schatte, G. in *Group 13 Chemistry: From Fundamentals to Applications*, (Eds.: Shapiro, P. J.; Atwood, D. A.) ACS Symposium Series 822, 2002.

46 (a) Brask, J. K.; Chivers, T.; Schatte, G. *Chem. Commun.* **2000**, 1805. (b) Chivers, T.; Fedorchuk, C.; Parvez, M. *Inorg. Chem.* **2004**, *43*, 2643.

47 Chivers, T.; Fedorchuk, C.; Schatte, G.; Parvez, M. *Inorg. Chem.* **2003**, *42*, 2084.

48 Chivers, T.; Fedorchuk, C.; Schatte, G.; Brask, J. K. *Can. J. Chem.* **2002**, *80*, 821.

49 (a) Cloke, F. G. N.; Dalby, C. I.; Daff, P. J.; Green, J. C. *J. Chem. Soc., Dalton Trans.* **1991**, 181. (b) Scoeller, W. W.; Grigoleit, S. *J. Chem. Soc., Dalton Trans.* **2002**, 405.

50 Chivers, T.; Fedorchuk, C.; Tuononen, H. M., *unpublished results.*

51 Chivers, T.; Fedorchuk, C.; Parvez, M. *Acta Crys.* **2005**, *C61*, o47.

52 For a review, see: van Koten, G.; Vrieze, K. *Adv. Organomet. Chem.* **1982**, *21*, 151.

53 Fernandes, J. A.; Sa Ferreira, R. A.; Pillinger, M.; Carlos, L. D.; Goncalves, I. S.; Ribeiro-Claro, P. J. A. *Eur. J. Inorg. Chem.* **2004**, *19*, 3913.

54 Denk, M.; Lennon, R.; Hayashi, R.; West, R.; Belyakov, A. V.; Verne, H. P.; Haaland, A.; Wagner, M.; Metzler, N. *J. Am. Chem. Soc.* **1994**, *116*, 2691.

55 Hermann, W. A.; Denk, M.; Behm, J.; Scherer, W.; Klingan, F. R.; Bock, H.; Soluki, B.; Wagner, M. *Angew. Chem., Int. Ed. Engl.* **1992**, *31*, 1485.

56 See, for example: (a) Warwel, S.; Wiege, B.; Fehling, E.; Kunz, M.; *Macromol. Chem. Phys.* **2001**, *202*, 849. (b) Grasa, G. A.; Hillier, A. C.; Nolan, S. P. *Org. Lett.* **2001**, *3*, 1077. (c) Grasa, G. A.; Singh, R.; Stevens, E. D.; Nolan, S. P. *J.*

Organomet. Chem. **2003**, *687*, 269. (d) Valente, A.; Moreira, J.; Lopes, A. D.; Pillinger, M.; Nunes, C. D.; Romao, C. C.; Kuehn, F. E.; Goncalves, I. S. *New J. Chem.* **2004**, *28*, 308.

57   See, for example: (a) Brown, D. S.; Decken, A.; Schnee, C. A.; Cowley, A. H. *Inorg. Chem.* **1995**, *34*, 6415. (b) Clyburne, J. A. C.; Culp, R. D.; Kamepalli, S.; Cowley, A. H.; Decken, A. *Inorg. Chem.* **1996**, *35*, 6651. (c) Brown, D. S.; Decken, A.; Cowley, A. H. *J. Am. Chem. Soc.* **1995**, *117*, 5421.

58   (a) Cui, C.; Roesky, H. W.; Schmidt, H.-G.; Noltemeyer, N.; Hao, H.; Cimpoescu, F. *Angew. Chem., Int. Ed.* **2000**, *39*, 4274. (b) Schmidt, E. S.; Jokisch, A.; Schmidbaur, H. *J. Am. Chem. Soc.* **1999**, *121*, 9758.

59   Arduengo, A. J., III; Harlow, R. L.; Kline, M. *J. Am. Chem. Soc.* **1991**, *113*, 361.

60   (a) Cloke, N. G. F.; Hanson, G. R.; Henderson, M. J.; Hitchcock, P. B.; Raston, C. L. *J. Chem. Soc., Chem. Commun.* **1989**, 1002. (b) Cloke, N. G. F.; Dalby, C. I.; Henderson, M. J.; Hitchcock, P. B.; Kennard, C. H. L.; Lamb, R. N.; Raston, C. L. *J. Chem. Soc., Chem. Commun.* **1990**, 1394. (c) Gardiner, M. G.; Raston, C. L.; Skelton, B. W.; White, A. H. *Inorg. Chem.* **1997**, *36*, 2795. (d) Pott, T.; Jutzi, P.; Neumann, B.; Stammler, H.-G. *Organometallics* **2001**, *20*, 1965. (e) Baker, R. J.; Farley, R. D.; Jones, C.; Kloth, M.; Murphy, D. M. *J. Chem. Soc., Dalton Trans.* **2002**, 3844. (f) Baker, R. J.; Farley, R. D.; Jones, C.; Kloth, M.; Murphy, D. M.; *Chem. Commun.* **2002**, 1196. (g) Pott, T.; Jutzi, P.; Kaim, W.; Schoeller, W. W.; Neumann, B.; Stammler, A.; Stammler, H.-G.; Wanner, M. *Organometallics* **2002**, *21*, 3169. (h) Antcliff, K. L.; Baker, R. J.; Jones, C.; Murphy, D. M.; Rose, R. P. *Inorg. Chem.* **2005**, *44*, 2098. (i) Baker, R. J.; Farley, R. D.; Jones, C.; Mills, D. P.; Kloth, M.; Murphy, D. M. *Chem. Eur. J.* **2005**, *11*, 2972.

61   See, for example: (a) Gardiner, M. G.; Hanson, G. R.; Henderson, M. J.; Lee, F. C.; Raston, C. L. *Inorg. Chem.* **1994**, *33*, 2456. (b) Kaupp, M.; Stoll, H.; Preuss, H.; Kaim, W.; Stahl, T.; van Koten, G.; Wissing, E.; Smeets, W. J. J.; Spek, A. L. *J. Am. Chem. Soc.* **1991**, *113*, 5606. (c) Abakumov, G. A.; Cherkasov, V. K.; Piskunov, A. V.; Druzhkov, N. O. *Dokl. Chem. Engl. Trans.* **2004**, *399*, 223.

62   Richter, S.; Daul, C.; von Zelewsky, A. *Inorg. Chem.* **1976**, *15*, 943.

63   Tuononen, H. M.; Armstrong, A. F., *unpublished results*.

64   *Diradicals*, (Ed.: Borden, W. T.), Wiley, 1998.

65   See, for example: (a) Berson, J. A. *Acc. Chem. Res.* **1997**, *30*, 238. (b) Dougherty, D. A. *Acc. Chem. Res*. **1991**, *24*, 88. (c) Rajca, A. *Chem. Rev.* **1994**, *94*, 871.

66   Abe, M.; Adam, W.; Heidenfelder, T.; Nau, W. M; Zhang, X. *J. Am. Chem. Soc.* **2000**, *122*, 2019.

67   See, for example: Amii, H.; Vranicar, L.; Gornitzka, H.; Bourissou, D.; Bertrand, G. *J. Am. Chem. Soc.* **2004**, *126*, 1344.

68   Nakano, M.; Kishi, R.; Nitta, T.; Kubo, T.; Nakasuji, K.; Kamada, K.; Ohta, K.; Champagne, B.; Botek, E.; Yamaguchi, K. *J. Phys. Chem. A.* **2005**, *109*, 885.

69   See, for example: Rodriguez, A.; Tham, F. S.; Schoeller, W. W.; Bertrand, G. *Angew. Chem., Int. Ed.* **2004**, *43*, 4876.

70   The theoretical treatment of diradicals in Section 3.1 is adopted from: Borden, W. T. in *Encyclopedia of Computational Chemistry* (Ed.: Schleyer, P. v. R.), Wiley, 1988, and from Reference 64.

71   For a discussion of Hund's rule in molecular systems, see: Hrovat, D. A.; Borden, W. T. *J. Mol. Struct. (Theochem)* **1997**, *398–399,* 211.

72   For a review of calculations on open-shell molecules, see: Bally, T.; Borden, W. T. in *Reviews in Computational Chemistry* (Eds.: Lipkowitz, K. B.; Boyd, D. B.), Wiley VCH, 1999.

73   See, for example: (a) Krylov, A. I.; Sherrill, C. D.; Head-Gordon, M.; Krylov, A. I. *J. Chem. Phys.* **1988**, *109*, 10669. (b) Krylov, A. I. *Chem. Phys. Lett.* **2001**, *348*, 375. (c) Krylov, A. I.; Sherill, C. D. *J. Chem. Phys.* **2002**, *116*, 3194.

74   Gritsenko, O. V.; Baerends, E. J. *Theor. Chem. Acc.* **1997**, *96*, 44.

75   Gräfenstein, J.; Kraka, E.; Filatov, M.; Cremer, D. *Int. J. Mol. Sci.* **2002**, *3*, 360.

76   For a review of recent developments, see: Gräfenstein, J.; Cremer, D. *Mol. Phys.* **2005**, *103*, 20.

77   (a) Schipper, P. R. T.; Gritsenko, O. V.; Baerends, E. J. *Theor. Chem. Acc.* **1998**, *99*, 329. (b) Schipper, P. R. T.; Gritsenko, O. V.; Baerends, E. J. *Chem. Phys.* **1999**, *111*, 4056.

78   (a) Filatov, M.; Shaik, S. *J. Phys. Chem. A* **2000**, *104*, 6628. (b) Filatov, M.; Shaik, S. *Chem. Phys. Lett.* **2000**, *332*, 409.

79   For a recent review, see: Grützmacher, H.; Breher, F. *Angew. Chem., Intl. Ed.* **2002**, *41*, 4006.

80   (a) Sita, L. R.; Kinoshita I. *J. Am. Chem. Soc.* **1990**, *112*, 8839. (b) Sita, L. R.; Kinoshita I. *J. Am. Chem. Soc.* **1991**, *113*, 5070. (c) Sita, L. R.; Kinoshita I. *J. Am. Chem. Soc.* **1992**, *114*, 7024.

81   (a) Jain, R.; Snyder, G. J.; Dougherty, D. *J. Am. Chem. Soc.* **1984**, *106*, 7294. (b) Jain, R.; Sponsler, M.; Coms, F. D.; Dougherty, D. *J. Am. Chem. Soc.* **1988**, *110,* 1356.

82   (a) Schoeller, W. W.; Dabisch, T.; Busch, T. *Inorg. Chem.* **1987**, *26*, 4383. (b) Schleyer, P. von R.; Sax, A. F.; Kalcher, J.; Janoschek, R. *Angew. Chem., Intl. Ed. Engl.* **1987**, *26*, 364. (c) Collins, S.; Dutler, R.; Rauk, A. *J. Am. Chem. Soc.* **1987**, *109*, 2564.

83   (a) Masamune, S. S.; Kabe, Y.; Collins, S. *J. Am. Chem. Soc.* **1985**, *107*, 5552. (b) Jones, R.; Williams, D. J.; Kabe, Y.; Masamune, S. *Angew. Chem., Intl. Ed. Engl.* **1986**, *25*, 173.

84   Schmidt, O.; Fuchs, A.; Gudat, D.; Nieger, M.; Hoffbauer, W.; Niecke, E.; Schoeller, W. W. *Angew. Chem., Intl. Ed.* **1998**, *37*, 949.

85   Niecke, E.; Fuchs, A.; Nieger, M. *Angew. Chem., Intl. Ed.* **1999**, *38*, 3028.

86   Niecke, E.; Fuchs, A.; Nieger, M.; Schmidt, O.; Schoeller, W. W. *Angew. Chem., Intl. Ed.* **1999**, *38*, 3031.

87   Sebastian, M.; Nieger, M.; Szieberth, D.; Nyulászi, L.; Niecke, E. *Angew. Chem., Intl. Ed.* **2004**, *43*, 637.

88   (a) Sugiyama, H.; Ito, S.; Yoshifuji, M. *Angew. Chem., Intl. Ed.* **2003**, *42*, 3802. (b) Ito, S.; Sugiyama, H.; Yoshifuji, M. *Phosphorus, Sulfur, Silicon Relat. Elem.* **2004**, *179*, 785.

89   Hommer, H.; Nöth, H.; Knizek, J.; Ponikwar, W.; Schwenk-Kircher, H. *Eur. J. Inorg. Chem.* **1998**, 1519.

90   (a) Jung, Y.; Head-Gordon, M. *J. Phys. Chem. A* **2003**, *107*, 7475. (b) Jung, Y.; Head-Gordon, M. *Chem. Phys. Chem.* **2003**, *4*, 522. (c) Cheng, M.-J.; Hu, C.-H. *Mol. Phys.* **2003**, *101*, 1319.

91   Walatka, V. V. Jr.; Labes, M. M.; Perlstein, J. H. *Phys. Rev. Lett.* **1973**, *31*, 1139.

92   Greene, R. L.; Street, G. B.; Suter, L. J. *Phys. Rev. Lett.* **1975**, *34*, 577.

93   For a recent review, see Banister, A. J.; Gorrell, I. B. *Adv. Mater.* **1998**, *10*, 1415.

94   (a) Mikluski, C. M.; Russo, P. J.; Saran, M. S.; MacDiarmid, A. G.; Garito, A. F.; Heeger, A. J. *J. Am. Chem. Soc.* **1975**, *97*, 6358. (b) Cohen, M. J.; Garito, A. F; Heeger, A. J.; MacDiarmid, A. G.; Mikluski, C. M.; Saran, M. S.; Kleppinger, J. *J. Am. Chem. Soc.* **1976**, *98*, 3844.

95   (a) Adkins, R. R.; Turner, A. G. *J. Am. Chem. Soc.* **1978**, *100*, 1383. (b) Findlay, R. H.; Palmer, M. H.; Downs, A. J.; Egdell, R. G.; Evans, R. *Inorg. Chem.* **1980**, *19*, 1307. (c) Skrezenek, F. L.; Harcourt, R. D. *J. Am. Chem. Soc.* **1984**, *106*, 3934. (d) Harcourt, R. D.; Skrezenek, F. L. *J. Mol. Struct. (Theochem)* **1987**, *151*, 203. (e) Harcourt, R. D.; Klapötke, T. M.; Schulz, A.; Wolynec, P. *J. Phys. Chem. A* **1998**, *102*, 1850. (f) Fujimoto, H.; Yokoyama, T. *Bull. Chem. Soc. Jpn.* **1980**, *53*, 800. (g) Gerratt, J.; McNicholas, S. J.; Karadakov, P. B.; Sironi, M.; Raimondi, M.; Cooper, D. L. *J. Am. Chem. Soc.* **1996**, *118*, 6472. (h) Thorsteinsson, T.; Cooper, D. *J. Math. Chem.* **1998**, *23*, 105. (i) Klapötke, T. M.; Li, J.; Harcourt, R. D. *J. Phys. Chem. A* **2004**, *108*, 6527. (j) Jung, Y.; Heine, T.; Schleyer, P. v. R.; Head-Gordon, M. *J. Am. Chem. Soc.* **2004**, *126*, 3132.

96   For a review, see: Gillespie, R. J.; Passmore, J. *Adv. Inorg. Chem. Radiochem.* **1971**, *4*, 413.

97   Saethre, L.; Gropen, O. *Can. J. Chem.* **1992**, *70*, 348.

98   (a) Schreckenbach, G.; Ruiz-Morales, Y.; Ziegler, T. *J. Chem. Phys.* **1996**, *104*, 8605. (b) Bühl, M.; Thiel, W.; Fleischer, U.; Kutzelnigg, W. *J. Phys. Chem.* **1995**, *99,* 4000.

99   Skrezenek, F. L.; Harcourt, R. D. *Theor. Chim. Acta* **1985**, *67*, 271.

100   Yamaguchi, K. *J. Mol. Struct. (Theochem)* **1983**, *12*, 101.

101   Hrovat, D. A.; Borden, W. T. *J. Am. Chem. Soc.* **1994**, *116*, 1512.

102   Kahn, S. D.; Hehre, W. J.; Pople, J. A. *J. Am. Chem. Soc.* **1987**, *109*, 1871.

103   Dutoi, A. D.; Jung, Y.; Head-Gordon, M. *J. Phys. Chem. A* **2004**, *108*, 10270.

104   (a) Hayes, E. F.; Siu, A. K. Q. *J Am. Chem. Soc.* **1971**, *93*, 2090. (b) Flynn, C.; Michl, J. *J. Am. Chem. Soc.* **1974**, *96*, 3280.

105   (a) Scholler, W. W.; Begemann, C.; Niecke, E.; Gudat, D. *J. Phys. Chem. A* **2001**, *105*, 10731. (b) Scholler, W. W.; Rozhenko, A.; Bourissou, D.; Bertrand, G. *Chem. Eur. J.* **2003**, *9*, 3611. (c) Ma, J.; Ding, Y.; Hattori, K.; Inagaki, S. *J.*

Org. Chem. **2004**, *69*, 4245. (d) Seierstad, M.; Kinsinger, C. R.; Cramer, C. J. *Angew. Chem., Intl. Ed.* **2002**, *41*, 3894.

106   (a) Kelly, P. F.; Slawin, A. M. Z. *Angew. Chem., Int. Ed. Engl.* **1995**, *34*, 1758. (b) Maaninen, A.; Laitinen, R. S.; Chivers, T.; Pakkanen, T. A. *Inorg. Chem.* **1999**, *38*, 3450.

107   Chivers, T. *A Guide to Chalcogen-Nitrogen Chemistry*, World Scientific, 2005.

108   Collins, M. J.; Gillespie, R. J.; Sawyer, J. F.; Schrobilgen, G. J. *Inorg. Chem.* **1986**, *25*, 2053.

109   (a) Lopez, X.; Sarasola, C.; Lecea, B.; Largo, A.; Barrientos, C.; Ugalde, J. M. *J. Phys. Chem.* **1993**, *97*, 4078. (b) Mühlhäuser, M.; Engels, B.; Ernzerhof, M.; Marian, C. M.; Peyerimhoff, S. D. *J. Phys. Chem.* **1996**, *100*, 120.

PAPER I

PAPER II

PAPER III

PAPER IV

PAPER V

PAPER VI